Electronics for Flow Through Electrode Capacitive Desalination

by

Liam Green

B.S. Electrical Engineering and Computer Science (2019)

Submitted to the Department of Electrical Engineering and Computer Science
in partial fulfillment of the requirements for the degree of

Master of Engineering in Electrical Engineering and Computer Science

at the

MASSACHUSETTS INSTITUTE OF TECHNOLOGY

May 2020

Author . . . .
Department of Electrical Engineering and Computer Science
May 12, 2020

Certified by . . . .
Steven Leeb
Professor of Electrical Engineering
Thesis Supervisor

Certified by . . . .
Steven Hunter
Lawrence Livermore National Laboratory
Thesis Supervisor

Accepted by . . . .
Katrina LaCurts
Chair, Master of Engineering Thesis Committee

Electronics for Flow Through Electrode Capacitive Desalination

by

Liam Green

Submitted to the Department of Electrical Engineering and Computer Science
on May 12, 2020, in partial fulfillment of the
requirements for the degree of
Master of Engineering in Electrical Engineering and Computer Science

Abstract

This thesis presents the design, construction, and testing of the power electronics, control circuit, and embedded system to facilitate a water desalination system that uses flow through electrode capacitive desalination technology. The focus is on designing, building, and testing the circuit that controls charging the electrodes that desalinate water and the circuit that recovers and stores the capacitive energy of the electrodes in order to improve the energy efficiency of the system. Multiple designs were considered in order to reduce cost, improve the feasibility of implementation, and improve energy efficiency of the system. The prototype electronic system was built and tested in a lab on a small scale setup with capacitive desalination cells. The feasibility of scaling up this system to a large scale desalination system was taken into consideration and is part of the goal of this project.

Thesis Supervisor: Steven Leeb
Title: Professor of Electrical Engineering

Thesis Supervisor: Steven Hunter
Title: Lawrence Livermore National Laboratory

Acknowledgments

Thank you to Steve Hunter, Steve Hawks, and Patrick Campbell for making this project possible and for their mentorship, support, and resources on this project at Lawrence Livermore National Laboratory. Thank you to everyone at Lawrence Livermore who assisted me with my work and who I had the pleasure to get to know during my time there. In addition, thank you to Steve Leeb for his help and feedback during my research and writing of this thesis.

Contents

List of Figures

List of Tables

Chapter 1

Introduction

In the United States, the availability of water has been identified as a national security concern that is relevant to the country's ability to meet its needs for water, agriculture, and energy [1]. Globally, over one billion people lack a reliable supply of fresh, clean water [1]. As the world's population continues to grow, this problem will worsen as the supply of fresh water shrinks with the increasing demand for its use around the world.

To solve this problem, water desalination systems are built to provide fresh water in areas that have access to saltwater, but have a scarcity of freshwater. Different desalination technologies are available, each with their own infrastructure, operation, maintenance, and energy costs associated with them. A newer desalination technology, known as capacitive desalination, has promising features that could make it competitive with currently used desalination technology. Here, capacitive desalination is compared with current desalination technology, its features and benefits are described, and promising applications for capacitive desalination are explored.

1.1 Water Desalination

98% of the water on the planet is sea water or brackish, i.e. slightly salty, and many cities around the world have built or are designing water desalination plants to address the issue of the scarcity of fresh water [4]. There are two main categories

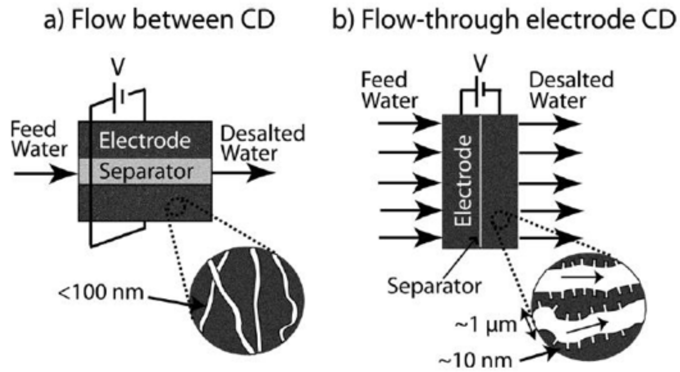

Figure 1-1: Schematics of capacitive desalination from [9]

for the most common water desalination methods: membrane-based, such as reverse osmosis, and thermal-based, such as multistage flash distillation [4]. The major costs of membrane-based desalination are the operational cost of membrane replacement and the energy cost of pumping water at a high pressure through the membranes, and the major cost of thermal-based desalination is the energy cost of heating the water [4]. In order to be competitive with these current methods, a desalination technology must have a low energy cost and a low cost of parts and maintenance.

1.2 Capacitive Desalination

Capacitive desalination (CD), also known as capacitive deionization (CDI), is a relatively new and potentially competitive technology for producing fresh water from sea or brackish water.

As seen in Figure 1-1(a), many capacitive desalination systems work by flowing saltwater between a pair of electrodes with an applied voltage [9]. The electric field between the electrodes from the applied voltage will move the positive sodium ions in the water to the negative electrode, and the negative chloride ions to the positive electrode. As these salt ions become trapped in the electrodes, the process reduces the salt concentration and produces less salty water.

A variation of this process as seen in 1-1(b) is to flow water through the porous carbon electrodes rather than through a separator between the electrodes. This method of flow through electrode capacitive desalination has been shown to produce a greater salt reduction in a shorter amount of time compared to the flow between method [9]. This research will focus on the electronics to support and implement a flow through electrode capacitive desalination system.

The advantages of capacitive desalination over reverse osmosis, the leading desalination method today, are that it does not require membranes to filter the salt from the water, it does not need to push water through the system at a high pressure, and it has the potential to use less energy [9]. The capacitive desalination electrodes eventually need to be replaced, and this cost is likely comparable to the membrane replacement cost for reverse osmosis. But capacitive desalination has the potential to operate at a lower cost because it does not need to use energy to pump water at high pressure through the system.

1.2.1 Energy Recovery

The flow through electrode desalination cell stores capacitive energy as a parallel plate capacitor. Currently this energy is lost when the electrodes are discharged during the flushing phase of the cycle. If this energy were transferred to another capacitor or battery for storage, power could be saved by reusing this energy to charge desalination cells or to power parts of the system.

There has been related work in using a buck-boost converter to recover this energy for capacitive desalination systems [8, 6]. The research for this project will include implementing and testing an energy recovery system for the flow through electrode capacitive desalination system. Different circuit topologies, such as a buck-boost converter and switched-capacitor converter, and different storage devices, such as capacitors and batteries, are considered.

1.3 Related Work

Atlantis Technologies is a company that has developed a Radial Deionization™ system that is a variation of capacitive desalination [11]. This system is a flow-between method of capacitive desalination, where water flows between a pair of separated electrodes along a relatively long path, allowing for more time and area for ions to be removed from the water [11]. The main applications for Atlantis Technologies' product are to desalinate water used for producing oil or generating power before it can be reused by recirculating through a boiler or before it can be discharged into the environment in order to meet environmental discharge regulations [11].

Voltea is a company that has developed a membrane capacitive deionization system, CapDI©, that is focused on removing ions from water with the ability to adjust the concentration of salt output by the system [12]. The applications for Voltea's technology include agriculture, industrial systems, consumer appliances, and residential buildings [12]. Their technology can be scaled up or scaled down based on the application and amount of water needed to be desalinated. For agriculture, their system can be adjusted to remove enough salt from water sources with a high enough salt concentration that would otherwise damage crops if used for irrigation. For industrial applications, their system can be used to remove enough minerals from water to avoid corrosion when water is used in industrial systems such as boilers and cooling towers, and can also be used to recover clean water from the waste water of industrial systems, such as laundry waste water. For consumer applications, their system can be used to provide clean water to appliances such as washing machines, dishwashers, and coffee machines. For residential applications, their system can be installed in one central location, such as an apartment building, that supplies clean water throughout the entire building [12].

1.4 Other Applications

Along with the application of producing clean drinking water and the applications of Atlantis Technologies' and Voltea's desalination systems, some recent research has focused on designing the carbon electrode material to selectively remove desired ions, such as nitrates or heavy metals, during the capacitive desalination process [10, 3]. This idea can be applied to design systems to remove specific known contaminants.

Capacitive desalination has a potential application in the coffee industry, with brewing coffee and espresso. Similar to some of Atlantis Technologies' and Voltea's applications, capacitive desalination can be used to remove minerals from water to avoid corrosion and scaling when the water is used in systems, which is relevant for avoiding excessive scaling in espresso machines. Additionally, when brewing coffee, a lot of effort is put into controlling the variables of the brewing process, such as water temperature, coffee grind size, water pressure, and flow rate, in order to produce the desired flavors in a way that can be repeated, and there is research focused on optimizing these variables [2]. It has also been shown that the dissolved minerals in water, such as sodium, magnesium, and calcium, affect the extraction of the flavor compounds from coffee beans, and [7] presents an ideal mineral composition of water for brewing coffee based on the chemistry of these dissolved minerals. When these minerals are dissolved in water, they form ions, Na^{+}, Mg^{2+}, and Ca^{2+}. A capacitive desalination system can be designed to remove a specific concentration of these ions so that the water has an ideal composition for extracting flavor from coffee. Making an espresso only uses 25-35 mL of water [2]; this low water volume usage would work well with the slow desalination rate of a capacitive desalination system. There are two companies, Third Wave Water and Global Customized Water, that sell products used for brewing coffee that add the desired mineral composition to filtered water used for brewing. Capacitive desalination can be applied to remove a desired concentration of minerals in water rather than adding a desired concentration. Outside of the coffee industry, this idea can be applied where the ion concentration of water plays an important role in a chemical process.

Chapter 2

Problem and Approach

This research is focused on the design of the electronics to support the research and implementation of a flow through electrode capacitive desalination system.

The electronics involve the controls, power electronics, and energy recovery for the system. The controls consist of the timing for the valves to control the flow of water into and out of the system, the timing for applying a voltage across the electrodes to control the desalination cycles, and the sensors for monitoring electric power, water pressure, and water conductivity. The power electronics consists of providing the required voltages to the desalination cells, valves, microcontroller, and system. The energy recovery electronics consists of a circuit to efficiently convert and store the electrodes' capacitive energy before the desalination cell is discharged.

The approach for this research was to design and build a prototype system to be used to test capacitive desalination cells, desalinating water on a relatively small-scale system in a lab. The process was to iterate on the design of the prototype system by adding more features, reducing cost, and making improvements. In addition, the energy recovery section of the system was researched and tested.

The next step will be to apply the research for this prototype system to install a larger system in a water desalination plant in California to implement and test the system on a large-scale application.

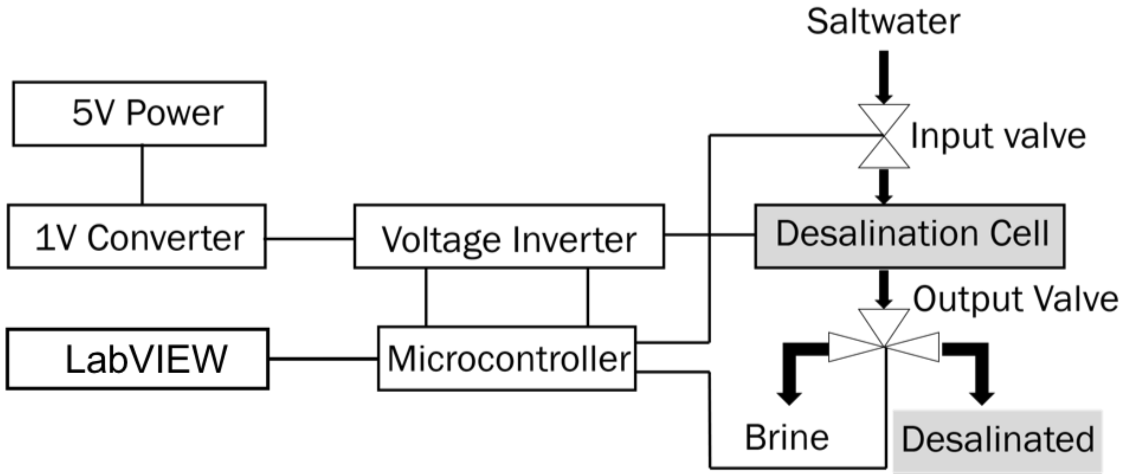

Figure 2-1: Block diagram of the prototype system

2.1 System

The diagram in Figure 2-1 shows the different parts of the system that need to be designed and built in order to implement a working prototype for a capacitive desalination system. As seen in the figure, saltwater flows into an input valve, through the desalination cell, and through an output valve that directs the water either to a brine collection or to a separate collection for desalinated water. A voltage inverter applies a voltage to the desalination cell, which determines whether the cell is desalinating the input saltwater and directing the output to the desalinated product collection or flushing trapped salt from the desalination cell and directing the concentrated salt solution to the brine collection. A microcontroller controls when the voltage across the desalination cell changes and when the states of the input and output valves change. A buck converter steps down the 5V system power to a lower voltage around 1V that the voltage inverter uses to apply to the desalination cell. A 5V power supply provides power to the microcontroller, the valves, and the 1V converter. A LabVIEW program communicates with the microcontroller to change the system controls through a user interface. The system and its components will be described in more detail in Chapter 3.

2.2 Requirements

A set of requirements and important features for the system are presented.

In order to be competitive with current desalination technologies, a major requirement for the system is to be low-cost. The objective is to minimize the costs associated with the parts, maintenance, operation, and energy required to build, maintain, and operate the system, especially taking into consideration how these costs would scale up to a larger system.

The system needs to cycle between charging the cell for desalination and discharging the cell to flush out trapped ions. Research has shown that alternating the polarity of the voltage applied to the cell for each charging cycle improves the performance of the cell compared to applying a voltage with the same polarity every cycle [5]. For this reason, the system must be able to cycle between a positive cell voltage, zero volts across the cell, and a negative cell voltage.

Capacitive desalination operates at a low voltage, around 1V, for charging the desalination cells. In order to test the effect of different charging voltages on ion removal, the system must be able to have an adjustable voltage supply in the range of around 0.8V to 1.4V. The higher the voltage, the more likely electrolysis will occur, producing hydrogen and oxygen gas, which is not efficient for desalination and can pose safety issues since hydrogen gas is flammable and oxygen gas accelerates combustion reactions. For this reason, it is desirable to have an adjustable low voltage supply around 1.0V.

The times for how long to charge the cells during the desalination phase and how long to discharge the cells during the flush phase must be able to be changed and controlled. This is an important feature in order to optimize the system to remove as much ion concentration as quickly as possible. If the desalination time is too long, then the trapped ions will begin to saturate in the electrodes, and the cell will remove less of the ion concentration. If the desalination time is too short, then the system suffers the cost of losing time and energy to switch to the flush cycle and using excess water to flush a smaller concentration of trapped ions. If the flush time is too long, then the system will waste water and time using more water than necessary to remove the trapped ions from the desalination cycle. If the flush time is too short, then the system will not remove all the ions from the cell and the cell will saturate more quickly when it switches to the desalination phase. The ability to control these times allows the system to be optimized to remove salt concentration without wasting excess water, time, or energy.

The time for switching the system's output valve is fixed at the time when the system switches to a different phase in the cycle, from desalination to flush and from flush to desalination. The output valve is switched to direct water to the desalinated product water during the desalination phase, and it is switched to direct water to the the concentrated waste water away from the desalinated water during the flush phase.

The time for the input valve must be able to be controlled for how long to switch to a slow flow during the flush phase. Slowing the speed of water during the flush phase reduces the amount of water it takes to flush the trapped ions. This increases the water recovery metric of the system, which is the ratio of volume of desalinated water to brine water. But reducing the flow rate will increase the amount of time it takes to flush the ions out of the cell, which reduces the amount of desalinated water the system can produce in a given amount of time since the system will spend a smaller proportion of time in the desalination phases. The ability to adjust how long to switch the input to a slow flow during the flush phase is desirable so that the system can be optimized and test the trade-offs of water flow speed during the flush phase.

An important feature of the prototype system to consider is the modularity of the system. While the prototype is tested on a few capacitive desalination cells in a lab, an important goal of this research is to install a scaled-up system in a desalination plant in California. Therefore, a modular design is preferable, where it is feasible to reliably scale up the prototype to a larger system that has the capacity to desalinate more water.

The system must also be compatible and interface with LabVIEW. This makes the system more user friendly and provides a standard interface and controls for the system that works with any computer with LabVIEW. It also makes the system compatible with existing sensors, like voltage sensors and conductivity sensors, that are used for testing in the lab.

Chapter 3

System Design and Overview

Based on the requirements and functionality of the capacitive desalination system, the electronics for the system were designed and built in order to create the functioning controls and power electronics to implement and test capacitive desalination. This design includes the power supplies for powering the system and charging the cells, how LabVIEW and a microcontroller interface with the system to control the circuit, and how the external components, such as the desalination cell and the valves, connect to the circuit and are controlled. The design choices are discussed and the design is documented so that the system can be recreated or adapted to meet new or different requirements for a specific capacitive desalination system. The way a user would setup and operate the system is also described.

3.1 System Overview

A diagram of the prototype design is shown in Figure 3-1. The 5V power supply is used to power the microcontroller, valves, and the MOSFETs that drive the high side MOSFETs of the full bridge inverter.

Signals from a microcontroller control the input and output water valves. The input valve switches between two states, as seen in the input water flow timing in Figure 3-2, controlling whether saltwater is flowing quickly or slowly into the desalination cell. The output valve is a three-way valve that controls where the output

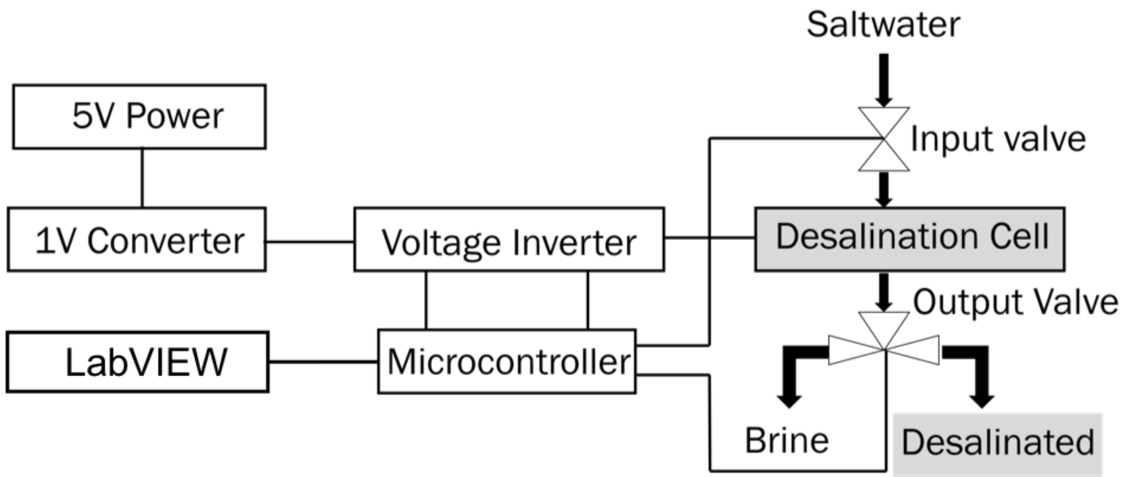

Figure 3-1: Block diagram of the prototype system

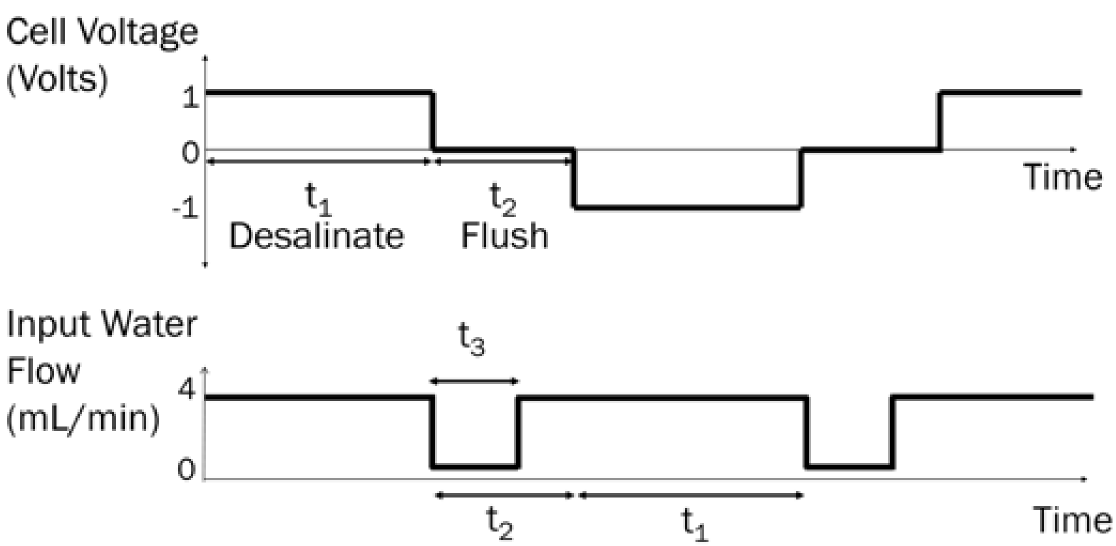

Figure 3-2: Timing for cell voltage and input water flow switching

water flows. When the cell is charged with a voltage and producing desalinated water, the output valve is switched to direct water to the desalinated product water. This phase is represented by the desalinate time t_1 in Figure 3-2. When the cell is flushing the trapped salt ions out of the cell and not producing desalinated water, the output valve is switched to direct water to the concentrated waste water away from the desalinated water collection. This phase is represented by the flush time t_2 in Figure 3-2. There is also a third time, t_3 in Figure 3-2, that is the length of time that saltwater is flowing slowly into the cells when the system switches from desalination to flushing. It is desirable to produce as little waste water as possible; therefore, the flow rate during the flush phase is slower in order to flush out the trapped ions with as little water as possible. The t_3 time can be the same length as t_2, in which case water will flow slowly for the entire duration of the flush phase. If t_3 is shorter than t_2, than water will flow slowly at the start of the flush phase for the duration of t_3. For the remaining time of the flush cycle, water will flow quickly. This provides the ability to adjust how long water is flowing slowly or quickly during the flush phase in order to balance the water-saving benefit of a slow flow with the time-saving benefit of a fast flow.

The applied voltage across the electrodes of the desalination cell needs to be around 1V, so a buck converter is used to step down the 5V system voltage to the 1V required for the cell. Alternating the polarity of the voltage decreases how quickly the electrodes degrade, so the desalination voltage alternates between +1V and -1V in order to improve the lifetime of the electrodes. The cell cycles between desalinating and flushing. The cell needs $\pm$1V during the desalination phase and 0V during the flushing phase, as seen in Figure 3-2. A full bridge inverter implemented with MOSFETs as seen in Figure 3-3 is used to achieve this voltage cycle by turning on and off the MOSFETs according to the control scheme in Table 3.1.

3.2 Power Supplies

To power the microcontroller, the valves, and the MOSFETs used to turn on the high side MOSFETs of the full bridge inverter, a 5V AC/DC power supply is used. This 5V supply is stepped down with a buck converter to charge the desalination cells with a lower voltage. A 30W 5V supply was chosen because the buck converter used in this prototype has a 20A max output current, which at 1.2V, the higher end of the voltage range for this application, consumes 24W of power. According to the MSP432P401R datasheet, the microcontroller consumes about 80μA of current in its active mode, its highest energy consumption operation mode. The valves each consume about 100mA of current when they are switched. The two MOSFETs used to turn on the high side MOSFETs of the full bridge inverter will allow at most 50mA to flow across each of the 100Ω resistors when they are on. At 5V, the total current required by the system, excluding the 1V converter, consumes about 1.5W.

$$5V(100mA + 100mA + 80\mu A + 50mA + 50mA) \approx 1.5W \tag{3.1}$$

The wattage for the 5V supply was chosen so that it provides enough power to meet the maximum total power, $P_{SYS-MAX}$, required by the 1V converter, valves, and microcontroller.

$$P_{SYS-MAX} = 24W + 1.5W = 25.5W \tag{3.2}$$

The 30 watts of the selected power supply provides more power than needed by the prototype system, and provides about 4.5W more power than required. With a system of more desalination cells with a higher max power consumption, a higher wattage 5V power supply would be required to provide enough power to the scaled up system.

The desired power supply for the desalination cell is an adjustable voltage supply in the range of 0.8V to 1.4V in order to test the desalination effectiveness at different applied voltage levels. A voltage higher than 1.4V will likely cause electrolysis, producing hydrogen and oxygen gas, which will not be efficient for desalination. The Analog Devices LTM4639 was chosen and used for this system because it has an output voltage range from 0.6V to 3.3V and has a high output current capability of 20A. This provides the ability to adjust the output voltage in the desired range for charging the desalination cells and can handle enough output current to charge about 20 desalination cells, since charging a single desalination cell draws about 1A peak current. The LTM4639 buck converter was also chosen because it is part of Analog Devices' μModule power module regulator series, which has a wide selection of power converters with different output current capabilities. This improves the modularity of the system, because if more current is needed to charge more cells in a larger system, then a different Analog Devices' μModule power module regulator can be selected that has a higher or lower output current capability. By designing the system to be compatible with this series of power converter chips, it simple to adjust the scale of the desalination system.

A demo board for the LTM4639 was used, which has the built-in ability to select an output voltage of 1.0V, 1.2V, 1.5V, or 1.8V. A resistor R_{FB} from the V_{FB} pin of the LTM4639 chip to ground programs the output voltage such that:

$$V_{OUT} = \frac{0.6V * (60.4k + R_{FB})}{R_{FB}} \tag{3.3}$$

As seen in Appendix Figure B-2, on the LTM4639 Demo Board, resistors R12, R13, R14, and R15 are the R_{FB} resistors that set the 1.0V, 1.2V, 1.5V, and 1.8V output voltages, respectively. These resistors can be swapped out with different values to set different output voltages. This board connects to the 5V supply and ground of the system and provides the lower output voltage to the voltage inverter. The connections for the LTM4639 board can be seen in Appendix Figure B-1.

3.3 Voltage Inverter

In order to achieve the desired voltages of +1V, 0V, and -1V to apply to the desalination cells, a full bridge inverter is used and implemented with MOSFETs, as seen in Figure 3-3. By turning the MOSFETs on or off according to the control scheme

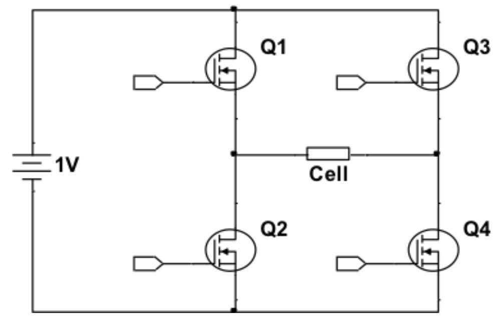

Figure 3-3: Full bridge inverter schematic

Cell Voltage	Q1	Q2	Q3	Q4
+1V	ON	OFF	OFF	ON
0V	OFF	ON	OFF	ON
-1V	OFF	ON	ON	OFF

Table 3.1: Full bridge inverter control scheme

in Table 3.1 with digital pins from the microcontroller, the desired cell voltage cycle can be achieved. This full bridge inverter topology eliminates the need for a second power supply with opposite polarity.

3.4 Circuit Schematic

A schematic of the circuit can be seen in Figure 3-4. The buck converter, labeled *A1*, is the LTM4639 that provides the 1V power supply to the full bridge inverter that is used to charge the desalination cells. MOSFETs *Q1*, *Q2*, *Q3*, and *Q4* form the full bridge inverter, similar to Figure 3-3, with a connection to provide the voltage to the cells. The IRL3803 MOSFET was selected as an inexpensive MOSFET for *Q1*, *Q2*, *Q3*, and *Q4*. This device has a max current capacity of 140A, much greater than the 20A max of the system. It has a low enough gate-to-source threshold voltage so that the 3.3V from the microcontroller pin can turn the MOSFET on. It also has a low on-resistance, which is important so that not much voltage is dissipated from drain to source during the high current desalination cell charging, since the drain voltage is already relatively low, about 1V. The switching period for the desalination system is on the order of minutes, so switching speed is not an important factor for

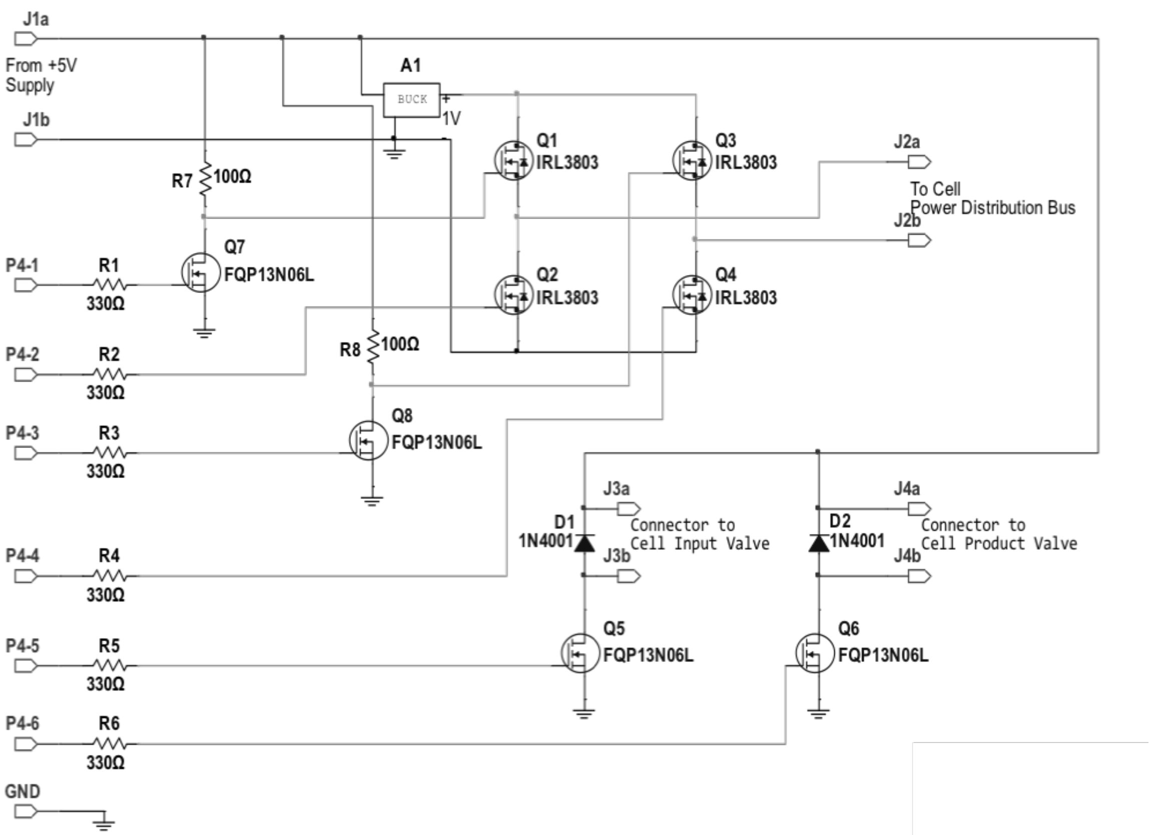

Figure 3-4: Circuit schematic

selecting MOSFETs in this circuit. Since the source pins of MOSFETs *Q1* and *Q2* of the full bridge inverter are not grounded, a higher gate voltage is needed to turn them on. MOSFETs *Q7* and *Q8* are used to provide this higher gate voltage. The FQP13N06L MOSFETs are used for *Q7* and *Q8* because this device is less expensive than the IRL3803 and has a low enough gate-to-source threshold voltage so that the 3.3V from the microcontroller pin can turn the MOSFET on. This device does not have as high of a current rating or as low on-resistance, which are not important since these MOSFETs are driving the gates of *Q1* and *Q3* rather than delivering high current to the desalination cells. On their drains, *Q7* and *Q8* are connected to the gates of *Q1* and *Q3* and to pull up resistors *R7* and *R8* to the 5V power supply. Therefore, when *Q7* and *Q8* are on, *Q1* and *Q3* gates are pulled low to ground, and *Q1* and *Q3* are off. When *Q7* and *Q8* are off, *Q1* and *Q3* gates are pulled high to 5V, and *Q1* and *Q3* are on. Labels *J2a* and *J2b* are the positive and negative connections to the positive and negative electrodes of the desalination cells connected in parallel.

The MOSFETs *Q5* and *Q6* are used to switch the input and output valves. The FQP13N06L MOSFETs are used for *Q5* and *Q6* for the same reasons they were selected for *Q7* and *Q8*. These valves use a solenoid as a switch. When *Q5* and *Q6* are on, current flows through the valve's solenoid and switches the state of the valve. Freewheeling diodes *D1* and *D2* are included to protect the MOSFETs *Q5* and *Q6* by dissipating current from the inductive load of the valves when the MOSFETs are turned off. Without the diodes, the current from the inductive load would dissipate across *Q5* and *Q6*, which can damage the MOSFETs over time. A 1N4001 diode is used for the diodes *D1* and *D2* because of its high forward surge capability and fast forward voltage drop, which allow it to quickly dissipate the inductive energy from the solenoids in the valves when *Q5* or *Q6* are turned off. Labels *J3a* and *J3b* are the positive and negative connections to the positive and negative terminals of the input valve. Labels *J4a* and *J4b* are the positive and negative connections to the positive and negative terminals of the output valve.

The connections *P4-1*, *P4-2*, *P4-3*, *P4-4*, *P4-5*, and *P4-6* are connected to digital output pins *P4.1*, *P4.2*, *P4.3*, *P4.4*, *P4.5*, and *P4.6* on the microcontroller, respectively, which are responsible for providing the signals to turn the MOSFETs on or off. The microcontroller digital signals output 3.3V when high, and the MOSFETs were chosen to have a low gate to source threshhold voltage such that they will turn on with a 3.3V gate voltage. Resistors *R1*, *R2*, *R3*, *R4*, *R5*, and *R6* are used to limit current flow when switching. When the microcontroller pins switch from high to low, the resistors limit the current flowing from the charged MOSFET gates, at 3.3V, into the low logic level pins, at 0V, in order to prevent damage to the pins. A 330Ω resistor will limit the current flowing into a pin on the microcontroller to 10mA, which is less than the max recommended current of 20mA from the MSP432P401R datasheet.

$$\frac{V_G - 0V}{R} = \frac{3.3V}{330\Omega} = 10mA \tag{3.4}$$

These resistors limit the switching speed of the MOSFETs, since it slows the speed of the MOSFET's gate charging up above the MOSFET's threshold votlage. But since the switching period for the system is on the order of minutes, switching speed is not an important aspect to consider.

A connection to the 5V AC/DC provides 5V to the full bridge inverter's high side MOSFETs, to the LTM4639 buck converter, and to the input and output valves. Labels *J1a* and *J1b* are the positive and negative connections to the 5V power supply, respectively. A barrel jack connector is used for this connection to allow the 5V AC/DC supply to easily plug into the circuit.

3.5 Circuit Picture

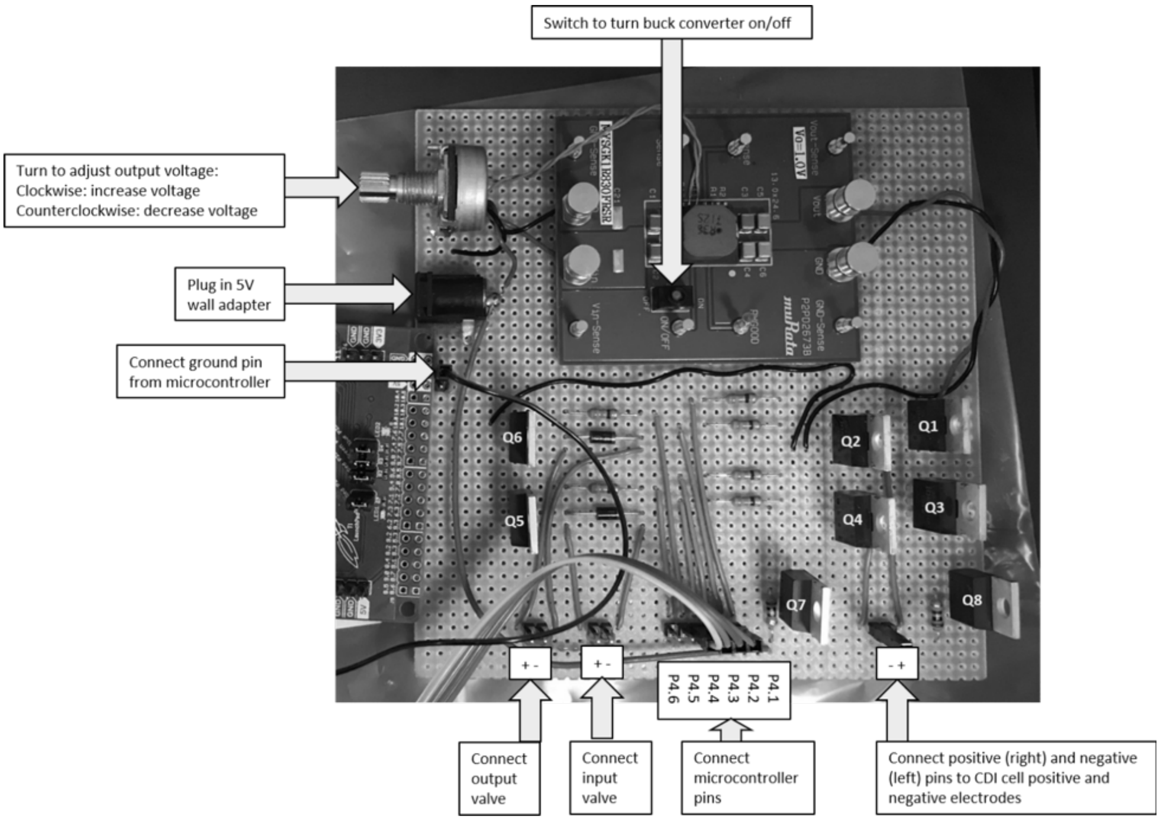

Figure 3-5: Prototype circuit on protoboard

Figure 3-5 shows a picture of the circuit built from the schematic in Figure 3-4 implemented on protoboard. This circuit uses the MYSGK1R830FRSR buck-converter chip to provide the 1V voltage to the full bridge inverter. This converter is similar to the LTM4639 and works for the system, but the next version of the desalination circuit uses the LTM4639 for the benefits mentioned in Section 3.2.

Figure 3-5 illustrates the connections to the microcontroller, valves, and desalination cells' electrodes.

3.6 Microcontroller

The Texas Instruments MSP432P401R microcontroller was chosen for its low power operating modes and its ease of use for programming and debugging. Digital signals

Cell Voltage	P4-1	P4-2	P4-3	P4-4
+1V	LOW	LOW	HIGH	HIGH
0V	HIGH	HIGH	HIGH	HIGH
-1V	HIGH	HIGH	LOW	LOW

Table 3.2: Microcontroller full bridge inverter control scheme

from this microcontroller operate the MOSFETs for the full bridge inverter and valves in the system. The software was programmed in C and debugged using Texas Instruments Code Composer Studio. Using UART and RS232, a user can send commands with a computer's USB to control the timings for the cell voltage cycle, timings for the valves, and the number of cycles to run. In order to save energy, the microcontroller remains in a low power operating mode most of the time, because much of the time it does not have to actively do anything. Interrupts using the microcontroller's timer are used to wake the microcontroller when it needs to send signals to change the state of the MOSFETs or valves. Interrupts are also used when a user sends commands to the microcontroller over USB.

3.6.1 Programming

To upload software to the MSP432P401R, jumper connectors must be on the RXD and TXD pins on the board. Code Composer Studio was used to edit, upload, and debug the software.

The main program for the software has two states: idle and desalination. During the idle state, the microcontroller is in a sleep mode until it receives a command to transition to the desalination state. During the desalination state, the microcontroller is switching the MOSFETs with digital output signals for the inverter and valves according to the chosen times for the desalinate, flush, and slow flow phases. While the microcontroller waits for the chosen amount of time before switching to the next phase of the cycle, it enters a sleep mode that is interrupted by a timer after the required amount of time. The microcontroller code for main.c can be seen in Appendix C.1.

3.6.2 Communication and Commands

To operate the system after uploading code to the microcontroller, P3.2 must be connected to the RXD pin. P3.3 must be connected to TXD pin on the MSP432P401R board.

Using UART and RS232, a user can send commands and receive messages with a computer's USB to control the timings for the cell voltage cycle, timings for the valves, and the number of cycles to run. Using a program like PuTTY, a user can use a terminal on their computer to connect to the serial port of their computer that the microcontroller is connected to. Once connected, a user can type commands that are sent over the serial connection to the microcontroller. When the microcontroller receives a command in its RX buffer, it triggers an interrupt that interrupts the microcontroller from the main program. The software handles the interrupt by performing some action based on what command was entered. The software updates any changes made to the system controls by the user's commands and returns to the main program. The microcontroller can also send messages using its TX buffer to the user's terminal over the serial connection.

To send a command, the user types # in their terminal to enter command mode. Then they enter the key corresponding to the command they want, followed by a value for the command. For example, a user can use this to change the length of time for the desalination phase.

When the microcontroller communication is not in command mode, the microcontroller is in status mode and will send messages about the status of the system based on the key the user input. For example, a use can get the status of the current length of time being used for the desalination phase.

A full list of commands can be seen in Appendix Table A.1

3.7 LabVIEW

LabVIEW virtual instruments were created for a user to operate the system with a simple front-end control panel. Three virtual instrument were created for the prototype lab testing to control the system, measure analog voltages, and measure conductivity of water flowing through the system.

The first virtual interface can be seen in Appendix Figure B-4. The VISA resource name is used to select the serial communication port that the microcontroller is connected to on the computer in order to establish a serial connection with the microcontroller, as is done when communicating with the microcontroller through a terminal. This interface can be used to select the desired times for desalinating, for flushing, and for the slow input water flow. The user can switch between the two system modes, idle or desalination, and select the number of charging cycles to run the system for. The instrument can also read in status information about the system, such as what state it is in, idle or desalination, and display this information on the interface. On the back-end of the instrument, the controls on the interface are programmed to send commands and receive messages from the microcontroller in the same way as communication through a terminal. When changing system settings, like the charge time, using the LabVIEW interface, the LabVIEW instrument sends the same command over the serial connection that a user would type in a terminal. The virtual instrument is initialized to be in the idle state, where the microcontroller output pins are set such that zero voltage is applied to the cells.

The second virtual instrument can be seen in Appendix Figure B-5. This interface is used to measure voltage signals using a National Instruments DAQ device connected to a USB port on the computer, that can convert analog voltage measurements into digital signals for LabVIEW to read and record. The DAQ has multiple analog input ports, and this LabVIEW virtual instrument can measure and record multiple voltage measurements. This virtual instrument can measure the desired voltages that are selected, which are each mapped to a specific positive and negative analog input pins on the DAQ. When the virtual instrument is run, the chart on the interface will graph the selected voltage measurements over time at the selected sample rate until the program is stopped. The voltage measurement data can be exported into Microsoft Excel or saved in a data format in order to save and record the data for analysis.

The third virtual instrument can be seen in Appendix Figure B-6. This is used to read measurements from a conductivity sensor that measures the conductivity of fluid flowing through it. The concentration of salt in the water can be computed using the conductivity measurement of the water, since salt concentration affects conductivity. The instrument is calibrated to calculate the sodium chloride concentration from the conductivity measurement and is calibrated to work with the conductivity measurement data of a Horiba 3574-10C Conductivity Cell (Flow Type) sensor. When the virtual instrument is run, the chart on the interface will graph the calculated salt concentration over time from the conductivity sensor data. This data can be exported into Microsoft Excel or saved in a data format in order to save and record the data for analysis.

3.8 PCB

A printed circuit board for the charging circuit was designed using Altium Designer, and can be seen in Appendix Figure B-7. A Bantam Tools PCB milling machine was used to manufacture the PCB from the Altium design files. The PCB starts off as a 4 in. x 5 in. FR-1 board with one side plated in copper. The milling machine mills away the copper surfaces that are not part of the PCB's traces and pads. The milling machine also cuts out the board outline and drills any holes in the board from the design files. A 1/32 in. flat end mill bit was used to make the PCB, so all traces, pads, and vias must be greater than 1/32 in. apart so that the mill bit has enough space to move between elements. Because the holes are not plated when making a PCB in this way, it is ideal to use surface-mount components for a better electrical connection rather than through-hole components. Surface-mount components must be chosen so that the solder pads for the components' packages are compatible with the requirement of not requiring any space between pads that are less than 1/32 in. apart. No trace widths are smaller than 10 mils so that traces are not too small, which would run the risk of disconnecting from the board as the bit mills the copper around them. The PCB was designed to have a smaller board outline than the maximum board size of 4 in. x 5 in. that the Bantam Tools machine can handle. This is done so that the machine cuts out the board outline from a 4 in. x 5 in. board, and then accurately mills the rest of the board relative to the outline. Therefore the board does not have to be perfectly aligned before starting the machine. The software on the Bantam Tools machine imports three design layer files from Altium: a top copper layer, a mechanical layer as the board outline, and a NC drill file for drill locations and holes.

A surface-mount D-PAK package was chosen for the MOSFETs because this package type is compatible with the layout spacing requirements of the Bantam Tools machine. Similarly, a 1206 (3216 metric) surface-mount package was chosen for the resistors and diodes. Referring to the PCB design in Appendix Figure B-7, the same resistors, 330Ω, and diodes, 1N4001, from the circuit schematic in Figure 3-5 are used for the PCB, in a 1206 surface-mount package size, for the same reasons as described in Section 3.4. The MOSFETs *Q1*, *Q2*, *Q3*, *Q4*, *Q5*, *Q6*, *Q7*, and *Q8* are IPD025N06N MOSFETs. These have similar characteristics as the IRL3803 MOSFETs described in Section 3.4, but the IPD025N06N MOSFETs were more readily available in the surface-mount D-PAK package.

Referring to the PCB design in Appendix Figure B-7, the label *P1* is a surface-mount connector for a barrel jack cable from the 30W 5V AC/DC power converter. The labels *P4-1*, *P4-2*, *P4-3*, *P4-4*, *P4-5*, *P4-6*, and *PGND* are surface-mount male pins that connect to the *P4.1*, *P4.2*, *P4.3*, *P4.4*, *P4.5*, *P4.6*, and *GND* pins on the microcontroller with jumper wires. The labels *P5* and *P6* are surface-mount male pins that connect to the input and output valve, respectively. Labels *J1*, *J2*, *J3*, *J4*, *J5*, and *J6* are banana jack connectors to easily connect to the LTM4639 demo board and to the CDI cells with cables with banana plugs.

A description of the connections to the PCB board can be seen in Appendix Figure B-8.

Chapter 4

Results

Two aspects of the capacitive desalination prototype system were tested: the basic functionality required for desalination and an energy recovery system that can be incorporated into the current circuit design with some modifications. For desalination testing, the system is setup so that saltwater flows into the desalination cells of the functioning system and the output of the desalination cells flows through a conductivity sensor to measure the salt concentration at the output. The voltage across the desalination cells' electrodes, the current into the electrodes, and the output salt concentration are measured over time while the system is operating. These measurements will show the electrical energy delivered to the desalination cells and the amount of salt concentration removed from the input saltwater. These measurements can be used to test the effectiveness of the system at desalination and to test the performance difference of different types of desalination cells used in the system. These measurements can also be used to adjust the duration of time for the desalination phase and the flush phase. The energy recovery test will test the feasibility and efficiency of transferring energy from a charged desalination cell. The results from this test can be used to determine the potential benefits and electricity cost savings, depending on the number of the desalination cells used in a system.

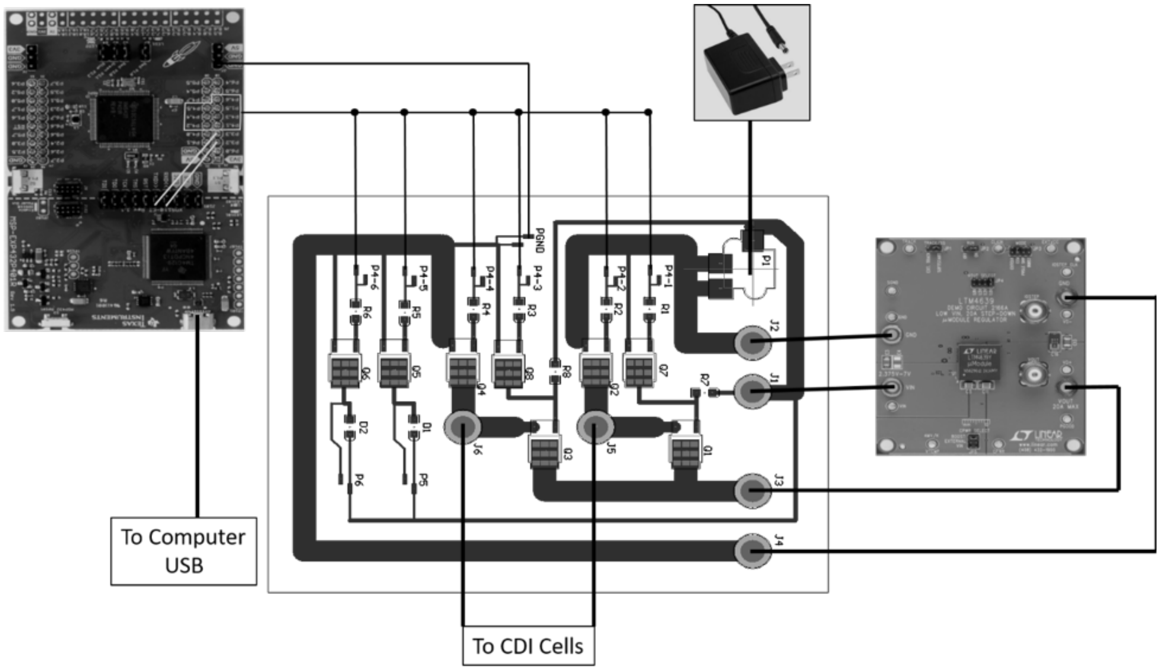

Figure 4-1: System Connections

4.1 Desalination

4.1.1 System Setup

The setup of the electronics can be seen in Figure 4-1. The LabVIEW virtual instruments are used to control the system, make measurements, and record data of cell voltage, cell current, and water salinity. A 0.56Ω power resistor is placed in series between the PCB connection to the cell and the cell's electrode. The voltage across this resistor is measured to calculate the current flowing into the cell. For testing, saltwater is pumped from a container into the desalination cells that are connected to the charging circuit. A conductivity sensor is placed at the output of the cells, that measures the conductivity of the water output by the cells over time. The output water flows back into the original container of saltwater.

4.1.2 Data Collected

Figure 4-2 shows data that was collected using one desalination cell with one full cycle of desalinating and charging the cell with 1V, flushing and applying 0V to the

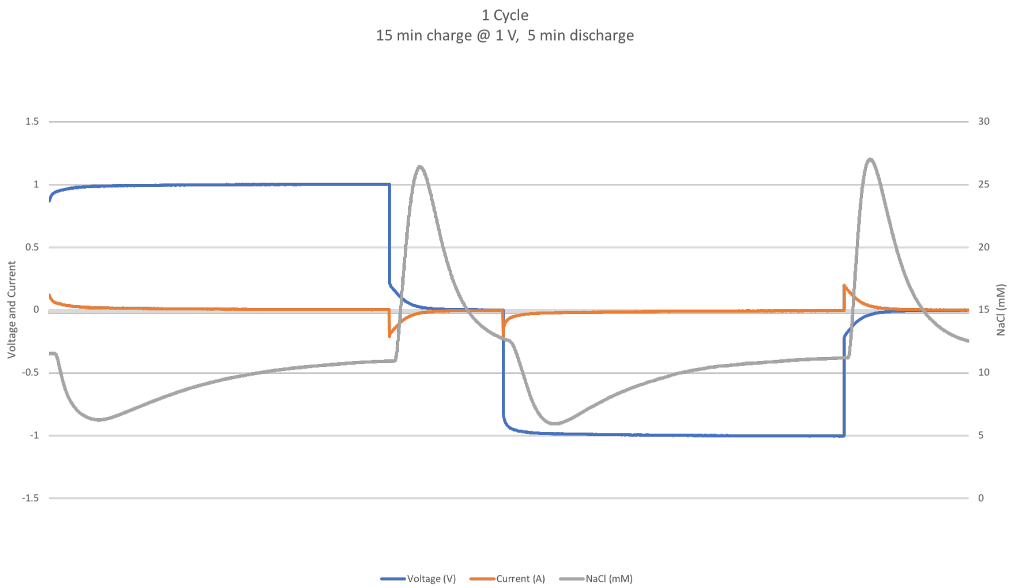

Figure 4-2: 1 Cycle of Capacitive Desalination

cell, desalinating and charging the cell with -1V, and flushing. As expected, the salt concentration in the water output decreases during the desalination phase and increases during the flush phase.

Figure 4-3 shows a comparison of the data collected using one desalination cell with one full cycle where the cell is charged with ± 1V compared to one full cycle where the cell is charged with ± 1.2V. As expected, more salt is removed when charging with a higher voltage since more energy is applied to the desalination cell to trap ions.

4.2 Energy Recovery

4.2.1 Motivation

The energy recovery testing is designed to research and test a method for quickly and efficiently saving the energy that is stored in a charged desalination cell, which has an equivalent energy storage capacity as a supercapacitor, before it is discharged during the flush phase. Rather than dissipate this energy by shorting the desalination cell's electrodes during the flush phase when zero voltage is applied to the cells, this testing

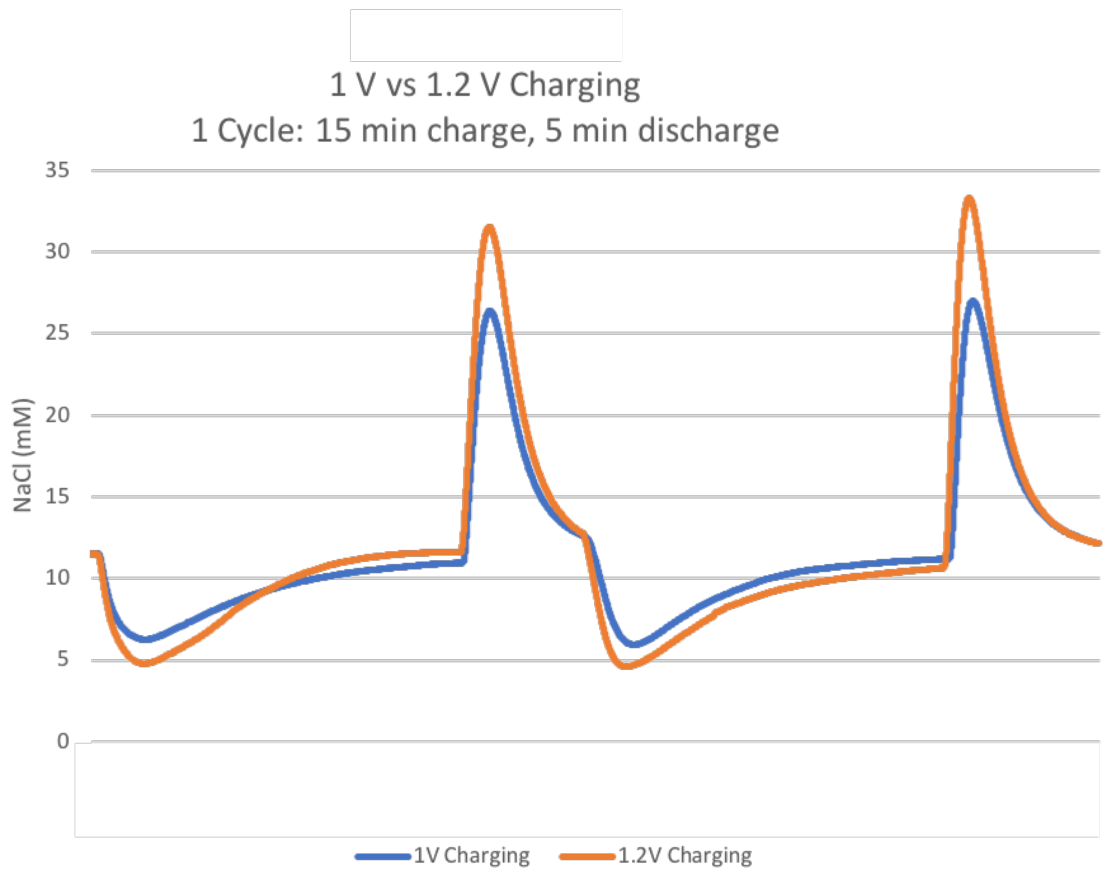

Figure 4-3: Effect of charging voltage on salt removal

will evaluate a method for saving the energy from a charged desalination cell that can be implemented in between the desalination phase and flush phase of the system. Using the simple energy transfer system of connecting an uncharged supercapacitor to a charged supercapacitor with a switch, as shown in Figure 4-4, only 25% of the initial energy stored in the charged supercapacitor can be transferred, which is shown in the derivation in Appendix D.1.

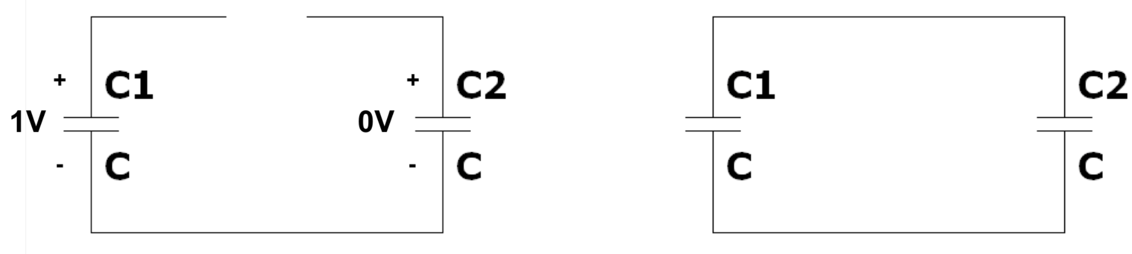

Figure 4-4: Initially C1 charged to 1V, C2 charged with 0V

This testing will evaluate using a buck-boost converter to more efficiently transfer energy so that a higher percent of the initial energy stored in a charged desalination cell can be saved. The energy recovery system can be implemented to transfer the energy from a charged desalination cell to charge another desalination cell or to store the energy in a supercapacitor or battery to be reused by the system. The benefit of implementing energy recovery is to save energy to reduce the cost of operating a capacitive desalination system and to reduce the environmental impact of consuming electricity. The cost savings of reducing electricity usage for this small prototype system is negligible. But the more the system is scaled up and the more desalination cells are used, an energy recovery system will have a greater impact on the electricity consumption of the system.

4.2.2 System Setup

To test the capability of energy recovery of a buck-boost converter on a desalination cell, this test charges a 1.2F supercapacitor with the same voltage that a desalination cell would have. The buck-boost converter converts the voltage from the charged supercapacitor to a constant voltage as the voltage of the supercapacitor drains. This constant voltage is dissipated across a 100Ω resistor, and the voltage across the resistor is measured. Eventually, as the voltage on the 1.2F supercapacitor approaches zero, the buck-boost converter will not be able to step up the supercapacitor voltage and maintain the constant voltage. Using the measured voltage across the resistor, this test will calculate the delivered energy to the resistor from the charged supercapacitor. Applying this constant voltage across the resistor from the buck-boost converter will simulate the energy transfer capability, and can be applied to use the constant voltage to charge another desalination cell, a supercapacitor, or a battery.

The Analog Devices LTC3110 chip was chosen to test the energy recovery capability of the system. It is a bidirectional buck-boost converter used to efficiently transfer energy from a supercapacitor used as a backup power supply for a system if the main system power supply fails. For this project it will be used to test the ability to transfer the energy from a charged desalination cell before the cell is discharged during the flush phase of the system. The LTC3110 steps up the V_{CAP} voltage from the charged supercapacitor or desalination cell to a higher voltage to power the load connected to V_{SYS} on the chip.

The LTC3110 demo board provides the choice of output voltage to V_{SYS} of 1.8V or 3.2V. 1.8V can be used to charge a supercapacitor. In order to provide the ability to charge a lithium battery with 4.2V, changes to the LTC3110 demo board were made and can be seen in Appendix Figures B-9 and B-10. The resistor values needed for the voltage calculation can be calculated from eq. 4.1 and eq. 4.2 from the LTC3110 datasheet in Appendix Figure B-11.

$$V_{SYS} = 0.6V(1 + \frac{R_{TOP}}{R_{BOT}}) \tag{4.1}$$

$$V_{CAP} = 1.095V(1 + \frac{R_{TOP}}{R_{BOT}}) \tag{4.2}$$

For V_{CAP}, R_{TOP} is set to 0 so that $V_{CAP} = 1.095V$, which is a voltage that can be used for a desalination cell. For V_{SYS}, $\frac{R_{TOP}}{R_{BOT}}$ is set to 6 so that $V_{SYS} = 4.2V$, which is

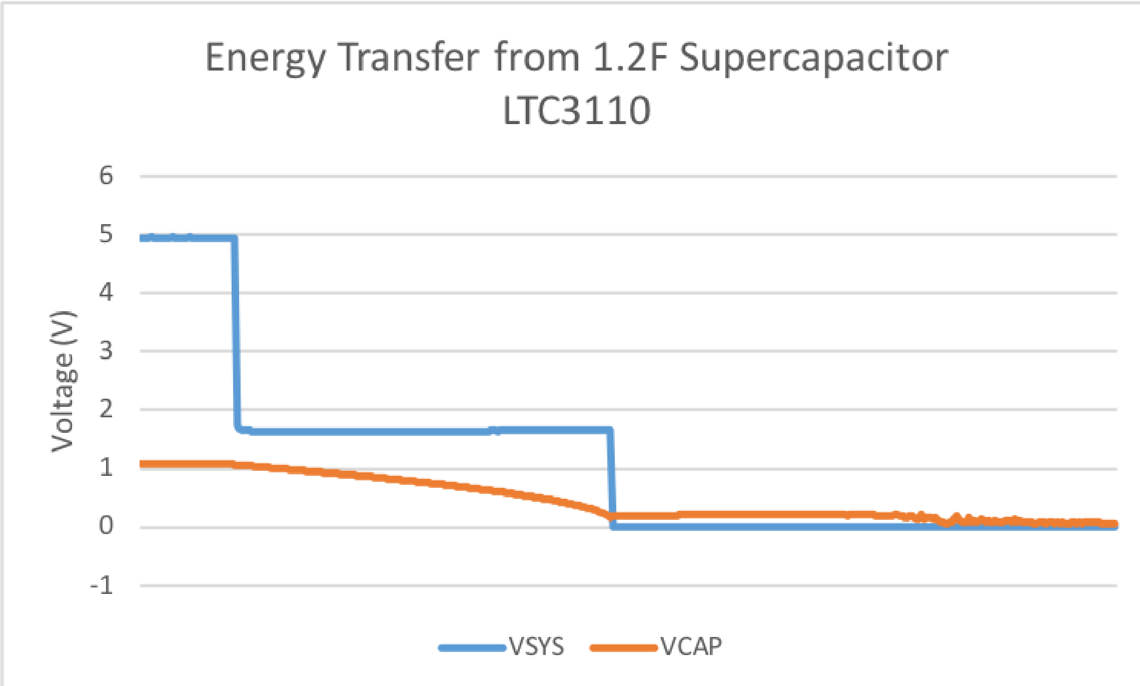

Figure 4-5: Energy recovery from 1.2F supercapacitor to 100Ω resistor

a voltage that can be used to charge a Li-ion battery. From the LTC3110 schematic in Appendix Figure B-10, these values can be achieved by changing $R10$ to 0Ω and $R5$ to $1.47M\Omega$.

This energy transfer system was tested by charging a 1.2F supercapacitor connected to V_{CAP}. A 5V power supply is used to power the chip. When the the 5V supply is connected and providing power, the LTC3110 keeps the supercapacitor charged. When the 5V power to the chip is removed, the LTC3110 automatically enters backup mode and transfers energy from V_{CAP} to maintain the desired voltage at V_{SYS}. For this test, V_{SYS} is connected to a 100Ω resistor and the output voltage to V_{SYS} is chosen to be 1.8V. The voltages across V_{CAP} and V_{SYS} were measured and recorded to evaluate how much energy can be transferred from the charged supercapacitor.

4.2.3 Data Collected

The 5 volts provided to V_{SYS} charges the supercapacitor to 1.1V. When the 5V supply is removed, the LTC3110 enters backup mode, and is designed to step up the supercapacitor voltage on V_{CAP} to 1.8V on V_{SYS}, where a 100Ω resistor is connected to ground. The voltage measurements of V_{SYS} and V_{CAP} over the time while the chip is in backup mode can be seen in Figure 4-5. The initial energy stored in the supercapacitor is calculated as E_C. From the raw voltage measurement data from Figure 4-5, the supercapacitor voltage was 1.07V before the LTC3110 switched to backup mode, which is used to calculate the initial energy.

$$E_C = \frac{1}{2}CV^2 \tag{4.3}$$

$$E_C = \frac{1}{2}(1.2F)(1.07V)^2 = 0.687Ws \tag{4.4}$$

The energy transferred to the resistor is calculated as E_R. From the raw voltage measurement data from Figure 4-5, the LTC3110 maintained 1.65V output from V_{SYS} for 15 seconds after the 5V power supply was disconnected.

$$E_R = \frac{V^2}{R} * time \tag{4.5}$$

$$E_R = \frac{(1.65V)^2}{100\Omega} * 15s = 0.408Ws \tag{4.6}$$

The ratio of energy provided to the resistor over the initial energy stored in the supercapacitor is calculated.

$$\frac{E_C}{E_R} = \frac{0.408Ws}{0.687Ws} = 0.594 \tag{4.7}$$

Therefore about 59.4% of the initial energy stored in the supercapacitor was able to be recovered as power delivered as a constant voltage to a resistor over time. This is a significant improvement over the simple two capacitor energy transfer system from Figure 4-4, which can only transfer 25% of the initial energy stored.

Chapter 5

Other Designs Considered

Other circuits were designed and built during the development of the final capacitive desalination prototype system. A discussion of these circuit designs is presented as well as details to why an alternative design was chosen in a subsequent iteration of the design. The final prototype system charges the desalination cells connected in parallel with a constant voltage. Other methods of charging the cells is discussed as well as why constant voltage charging in parallel was ultimately chosen.

5.1 Previous Circuit Designs

5.1.1 Voltage Polarity Switching with Relays

Figure 5-1 shows the schematic for a previous circuit design to implement the system. Here, a pair of DPDT relays are used to achieve the voltage polarity switching required for the desalination cycle. Relay 1 switches whether +1V or -1V is applied to the cell electrodes. Relay 2 switches whether the ±1V or 0V is applied to the cell electrodes. Appendix Figure B-13 shows a picture of this system.

A connection to the 30W 5V AC/DC power supply provides 5V to power the relays, the buck converter, and the input and output valves. Labels *J1a* and *J1b* are the positive and negative connections to the 5V power supply, respectively. A barrel jack connector is used for this connection to allow the 5V AC/DC supply to easily

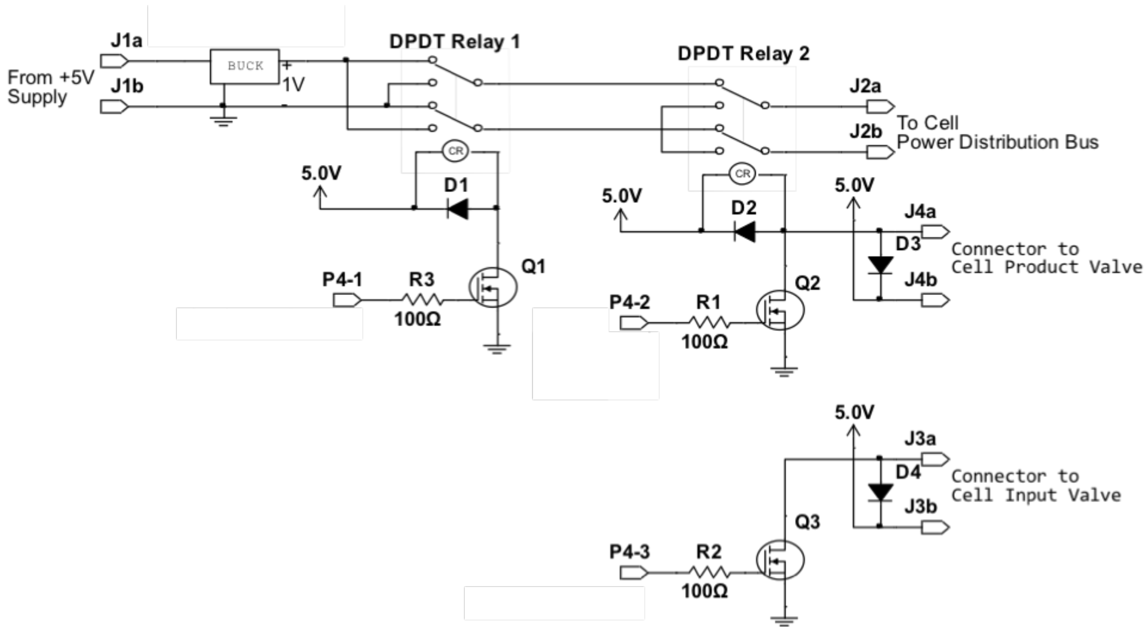

Figure 5-1: Circuit schematic of electronics prototype system

plug into the circuit.

The connections *P4-1*, *P4-2*, and *P4-3* are connected to digital output pins *P4.1*, *P4.2*, and *P4.3* on the microcontroller, respectively, which are responsible for providing the signals to turn the MOSFETs on or off.

The MOSFETs *Q1*, *Q2*, and *Q3* are FQP13N06L MOSFETs used for the same reason as described in Section 3.4. Turning on *Q1* will switch Relay 1 to reverse the polarity and apply -1V to the desalination cells. Turning on *Q2* will switch Relay 2 to short the electrodes of the desalination cells and switch the output valve state so that it is directed to the brine collection. Turning on *Q3* will switch the input valve to be in the slow flow state. 100Ω resistors *R1*, *R2*, and *R3* are used to limit the current flow into the microcontroller pins, *P4.1*, *P4.2*, and *P4.3*, when the MOSFETs *Q1*, *Q2*, or *Q3* are turned off. The resistors limit the current flow from the charged MOSFET gates at 3.3V into the low level microcontroller pins at 0V, so that the pins are not damaged by sinking too much current. 100Ω was not a sufficiently large resistance, and some of the microcontroller pins were damaged with this circuit. These resistances were increased in the final circuit design to prevent this damage. Diodes *D1*, *D2*, *D3*, and *D4* are freewheeling diodes included to dissipate current from the inductive relay coils and valve solenoids when the MOSFETs are turned off. 1N4001 diodes are used for the same reason as described in Section 3.4.

Labels *J2a* and *J2b* are the positive and negative connections to the positive and negative electrodes of the desalination cells connected in parallel. Labels *J3a* and *J3b* are the positive and negative connections to the positive and negative terminals of the input valve. Labels *J4a* and *J4b* are the positive and negative connections to the positive and negative terminals of the output valve.

This system worked as expected and successfully produced the controllable +1V, 0V, and -1V voltages for the desalination cells. The final circuit designed for this project used a full bridge inverter implemented with MOSFETs rather than a pair of DPDT relays, because the full bridge inverter is cheaper and smaller compared to a pair of DPDT relays, which are beneficial characteristics for scaling up the system for a large-scale desalination plant. This circuit uses the MYSGK1R830FRSR buck converter chip to provide the 1V voltage to the full bridge inverter. This converter is similar to the LTM4639 and works for the system, but the final version of the desalination circuit uses the LTM4639 for the benefits mentioned in Section 3.2.

5.1.2 Protoboard Circuit

Appendix Figure B-12 shows a picture of a previous prototype system design that implements a full bridge inverter with MOSFETs and has the same circuit design as the final PCB circuit for this project. This previous circuit was built on a protoboard.

This system worked as expected and successfully produced the controllable +1V, 0V, and -1V voltages for the desalination cells. The final circuit designed for this project is built on a PCB rather than on a protoboard. One advantage of a PCB is that it can easily be reproduced by using the same PCB design files. The PCB is made and the components are soldered on. This is a quicker and more reliable process than using a protoboard. Since components have to be soldered together with individual wires rather than traces on a PCB board, it is more likely that mistakes will be made when reproducing the circuit and wires can more easily become disconnected. Another advantage of a PCB is that it makes the system more modular. To scale up the system, more PCBs have to be made, which is easier and quicker than having to manually wire up multiple protoboards as the system scales.

5.2 Power Delivery

5.2.1 Constant Current Charging

The final prototype system for this project uses constant voltage charging, where the 1V voltage supply is applied to the desalination cells. Another method that could be used is constant current charging, where a current source is used to charge the desalination cells. Constant voltage charging was chosen for the system because it is simpler to implement, which is an important factor as the system scales up.

5.2.2 Series Charging

The final prototype system for this project charges desalination cells in parallel by applying ±1V across all the cells. Another method that could be used is to charge the cells in series with a higher voltage rather than in parallel. For example, a 5V power supply could be connected across 5 desalination cells in series, so that there will be 1V across each desalination cell's electrodes. But this will only be the case if all the cells have the same properties, such a series resistance and capacitance. If the cells are not perfectly matched, then there will be different voltages across different cells, which will cause different rates of desalination and can damage a cell if its voltage is too high. Because of these complications, parallel charging was chosen for the design of the electronics.

5.2.3 Pulsed Voltage Wave Charging

Because the capacitance of the desalination cell is very high, the cell acts like a low-pass filter to a voltage applied to its electrodes. In theory, the voltage across the cell will be the average of the voltage applied. Using this idea, a cheap way to power the cells during charging would be to rectify an AC voltage with a diode such that the average voltage of that rectified wave is 1V. Because of the nature of the carbon material that is used, it is likely that applying pulses of a high voltage from a rectified AC voltage will damage the material and negatively affect its ability to desalinate. Because of this, a constant low voltage power supply is used for charging the cells.

Chapter 6

Future Work and Improvements

A goal of this project is to install a a larger version of this prototype system in an actual desalination plant in California. The work for this project is not only for research purposes, but also for a real commercial need for this new water desalination technology. A significant part of the design and planning of the electronics for this system took into consideration the requirements to ensure that this system works reliably, effectively, and efficiently in an actual water desalination facility. Because the prototype discussed in this thesis is part of an ongoing project, it is important to make improvements and explore possible changes to the system for better performance, easier use and implementation, and for a more competitive and complete commercial product that can be used to challenge existing desalination technologies and improve the world's ability provide a sufficient and reliable source of fresh water. Some suggested improvements are presented here.

6.1 LabVIEW Improvements

Currently there are three separate LabVIEW virtual instruments. An improvement to this system would be to combine these into one LabVIEW interface. By having all the controls and displays in one interface, the system would be easier to use and monitor the desalination tests.

Another improvement to the LabVIEW interface would be to have more information about the system displayed during the desalination process. For example, it would be useful to display the current output voltage, states of the valves, and timings for the desalination and flush phases.

6.2 Additional Sensors

A current sensor would be useful to monitor the power used by the system. The current measurement can be sent to the LabVIEW interface for real-time power monitoring of the whole system or of the power delivered to the desalination cells.

Additional sensors, such as flow rate and water pressure would be useful to have when the system is installed in a large desalination plant. These sensors can be used to detect if one or more of the desalination cells are clogged or leaking. This can be used to send an alert that all the cells are not functioning properly or it can be used to implement an automatic shut-off feature to shut-off the input to a cell that is not functioning correctly so that it does not negatively impact the efficiency of the whole system.

6.3 Output Voltage

Currently the LTM4639 Demo Board used in this system provides the voltage output option of 1.0V, 1.2V, 1.5V, or 1.8V. A resistor R_{FB} from the V_{FB} pin of the LTM4639 chip to ground programs the output voltage such that:

$$V_{OUT} = \frac{0.6V * (60.4k + R_{FB})}{R_{FB}} \tag{6.1}$$

As seen in Appendix Figure B-2, on the LTM4639 Demo Board, resistors R12, R13, R14, and R15 are the R_{FB} resistors that set the 1.0V, 1.2V, 1.5V, and 1.8V output voltages, respectively. These resistors can be swapped out with different values to set different output voltages. An improvement to the system would be to use a digital potentiometer as the R_{FB}, whose resistance is controlled by the microcontroller. This feature can be combined with an additional microcontroller command that allows the user to control the output voltage used to charge the desalination cells by digitally controlling the value of R_{FB}. This can be added to the LabVIEW interface with the other system controls.

6.4 Energy Recovery

The energy recovery capability of the circuit was tested with the LTC3110 demo board by charging up a supercapacitor and then transferring the voltage from the supercapacitor to a resistor in order to measure how much energy was able to be transferred. The next step would be to incorporate the LTC3110 into the current circuit design and add an additional mode to the system in between the desalination and flush phases where energy is trnsferred from the charged cells to a storage device.

6.5 PCB Improvements

The next improvement to the PCB design would be to transition the current design to a 2-sided PCB. This would allow through-hole components to be used where necessary since the vias would be plated and provide a good electrical connection, unlike the one-sided PCB. Using through-hole versions of the male header pins and the barrel jack connector would provide a more secure mechanical connection when plugging wires into these components. A 2-sided PCB version would also allow the layout to be designed to have shorter and wider traces for the 1V supply and the ground. The current design has relatively long and narrow traces, which increases the resistance of the path. Having shorter and wider traces would reduce voltage dissipated by the resistance of the traces, especially for the high current application of charging desalination cells.

Another improvement for the PCB, and the system in general, is to expand on the current PCB design to also include the microcontroller and the buck converter on the PCB. Currently there are wires connecting the pins of the PCB to the pins of the microcontroller board and banana cables connecting the PCB to the LTM4639 demo board. Rather than having these three separate circuit boards, a simpler design would be to incorporate all of them into one board.

6.6 System Operation

The capacitive desalination method used for this project operates in a single pass. Input water makes a single pass through the desalination cells and enough ions are removed such that the output product is at the desired salt concentration level. A different, and potentially better, way to operate the system is in a batch mode. In this mode of operation, the output of the cells flows back to the input so that more salt can be removed each time it passes through the cells. In this way, a batch of water is cycled through the system, removing salt over time until a desired concentration is reached, at which point the water will leave the system into the desalinated water product and a new batch of saltwater enters the system to be desalinated. In order to explore the effectiveness of this mode of operation, modifications can be made to the current system to implement support for a batch mode.

Chapter 7

Conclusion

This thesis presents the design of the electronics necessary to implement a flow through electrode capacitive desalination system. The requirements and desired features for the system are described, and a prototype system that was designed and tested is presented that meets these requirements and implements the desired features. This prototype system describes the power electronics, control circuit, and embedded system built and tested to facilitate a desalination system that uses flow through electrode capacitive desalination technology. The system was successfully able to desalinate water in a lab as expected. The system also tests the potential for energy savings by recovering the stored electrical energy from the desalination cells. The design of the system focuses on making capacitive desalination technology competitive with current technologies by reducing the cost and increasing the feasibility of scaling the system up so that it can be implemented in a larger-scale desalination plant in California. This system, with improvements, has the potential to be a reliable and economical source of water desalination.

Appendix A

Tables

Key	Command Mode Description	Status Mode Description
g	Input new command code, 0 = Idle, 3 = Desalination Cycle	Returns current command being executed
n	Change the number of desalination cycles for batch mode	Returns the last set number of cycles for batch cycle
x	Set slow input flow time	Returns last set slow input flow time
y	Set charging time	Returns last set charging time
z	Set discharging time	Returns last set discharging time
0-9	Numerical input for other commands	
.	Decimal input for other commands	
#		Enters command mode
ESC	Exit from command mode or commands that require numerical input	
BKSP	Allows for the deletion of the last input character	
ENTER	Commits selected command	Inserts newlines into terminal

Table A.1: Terminal commands

Appendix B

Figures

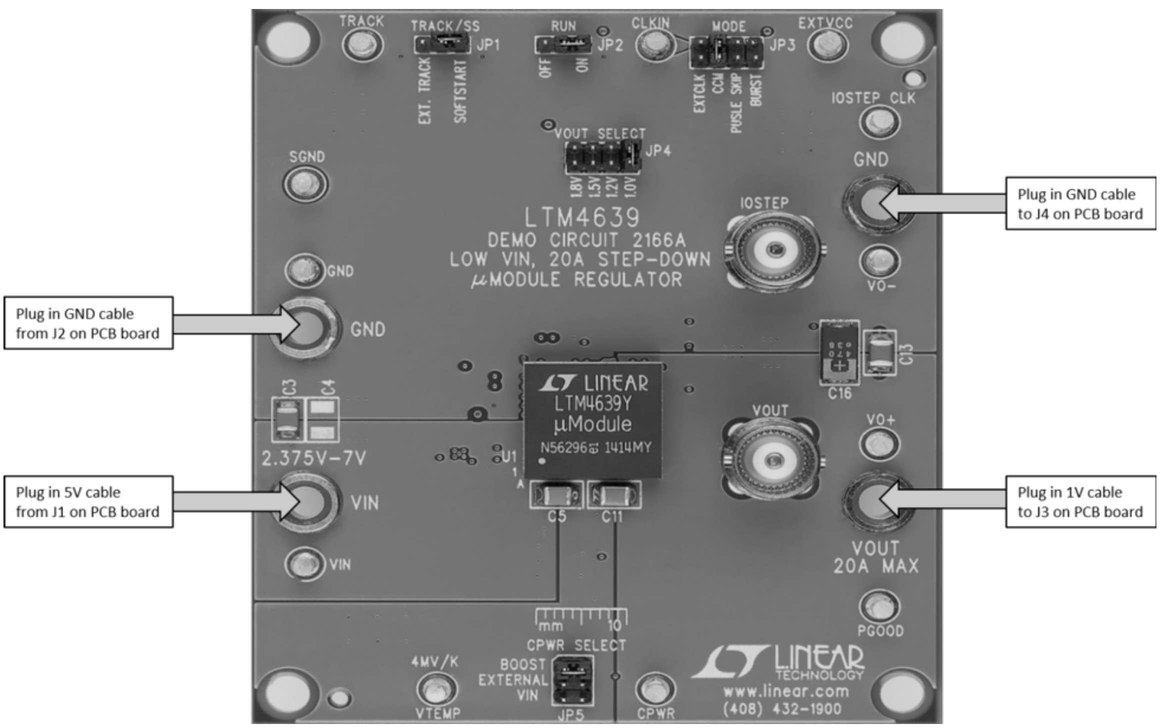

Figure B-1: Connections for the Buck Converter Board

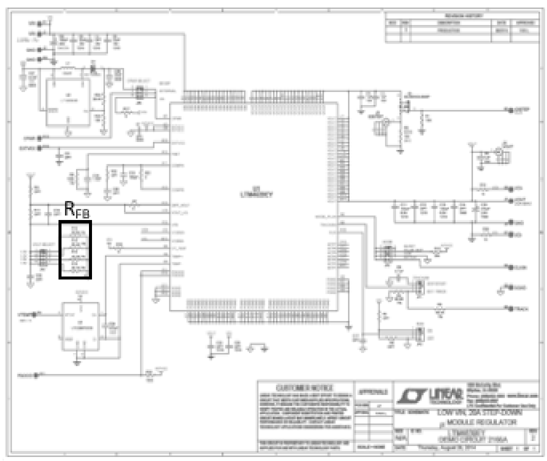

Figure B-2: Modifying output voltage for LTM converter

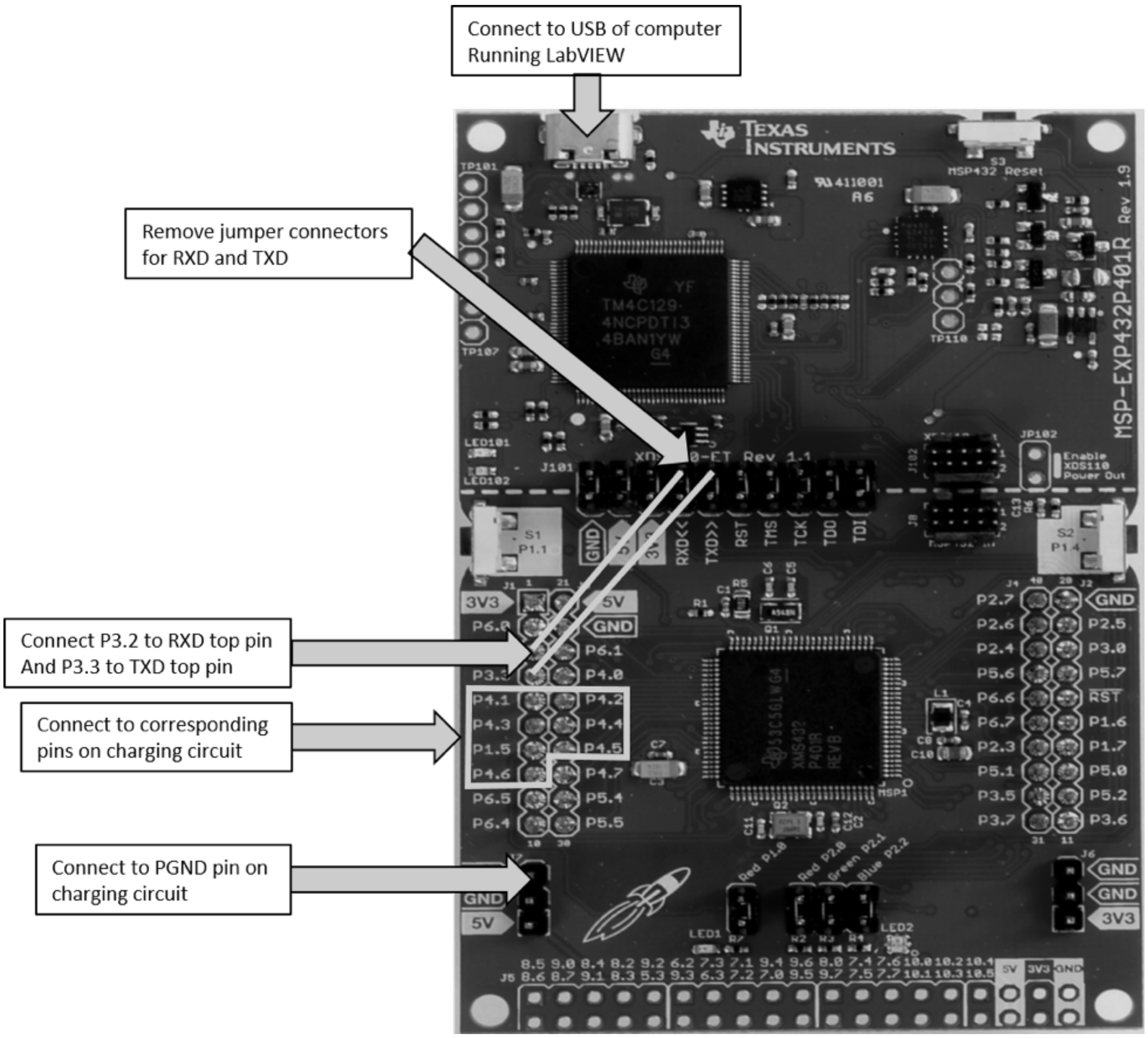

Figure B-3: Microcontroller Connections

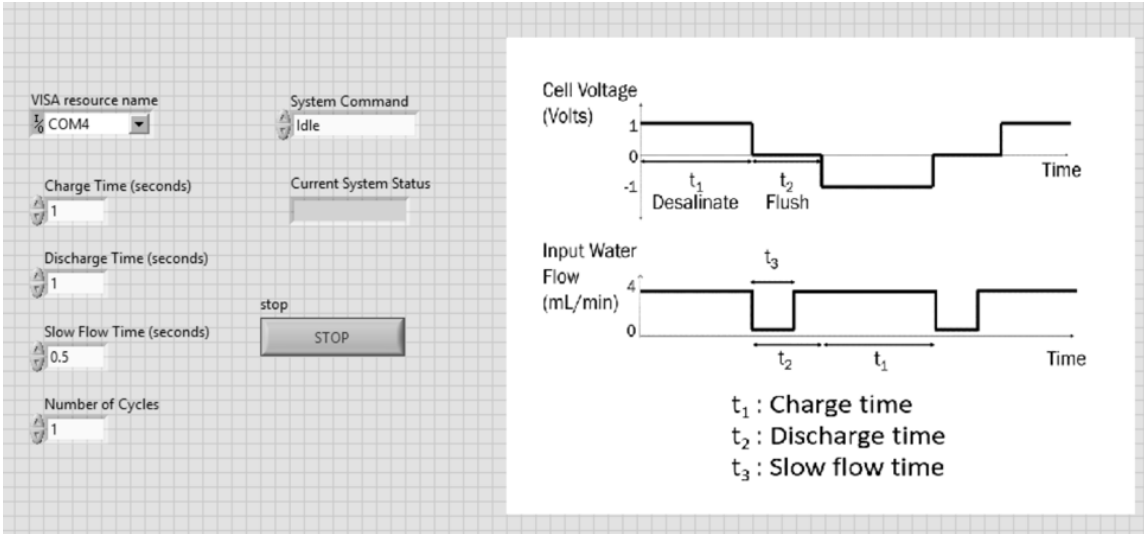

Figure B-4: LabVIEW SimpleInterface.vi

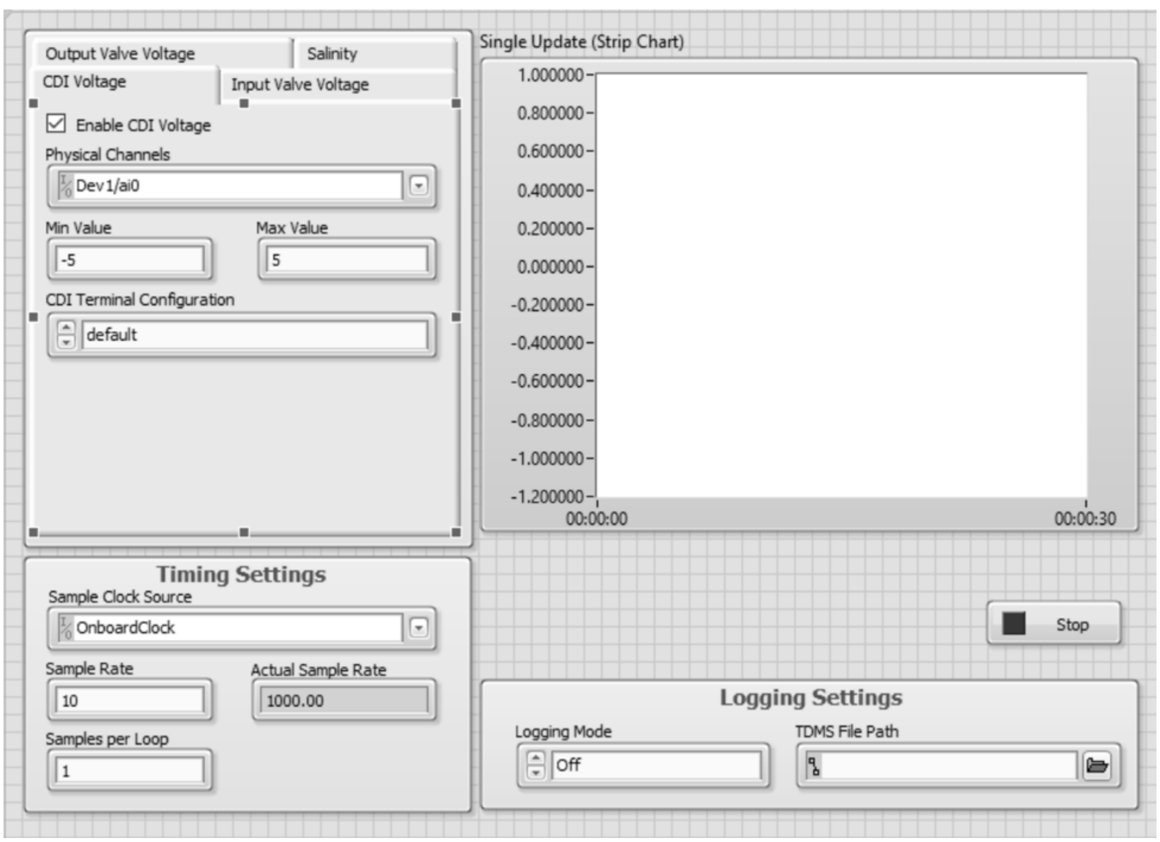

Figure B-5: LabVIEW AnalogInput.vi

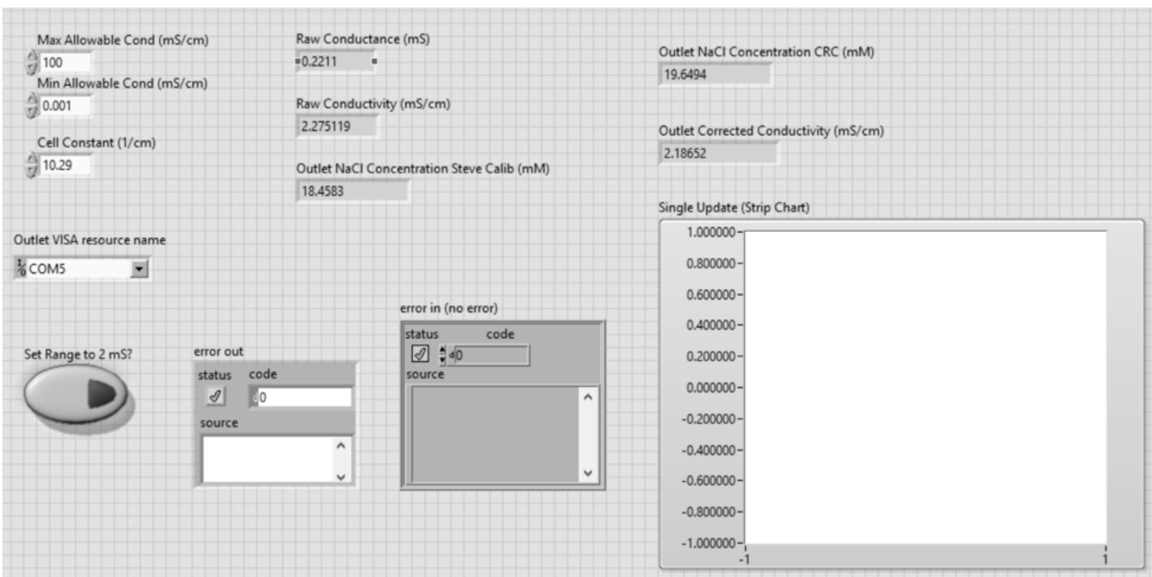

Figure B-6: LabVIEW Conductivity.vi

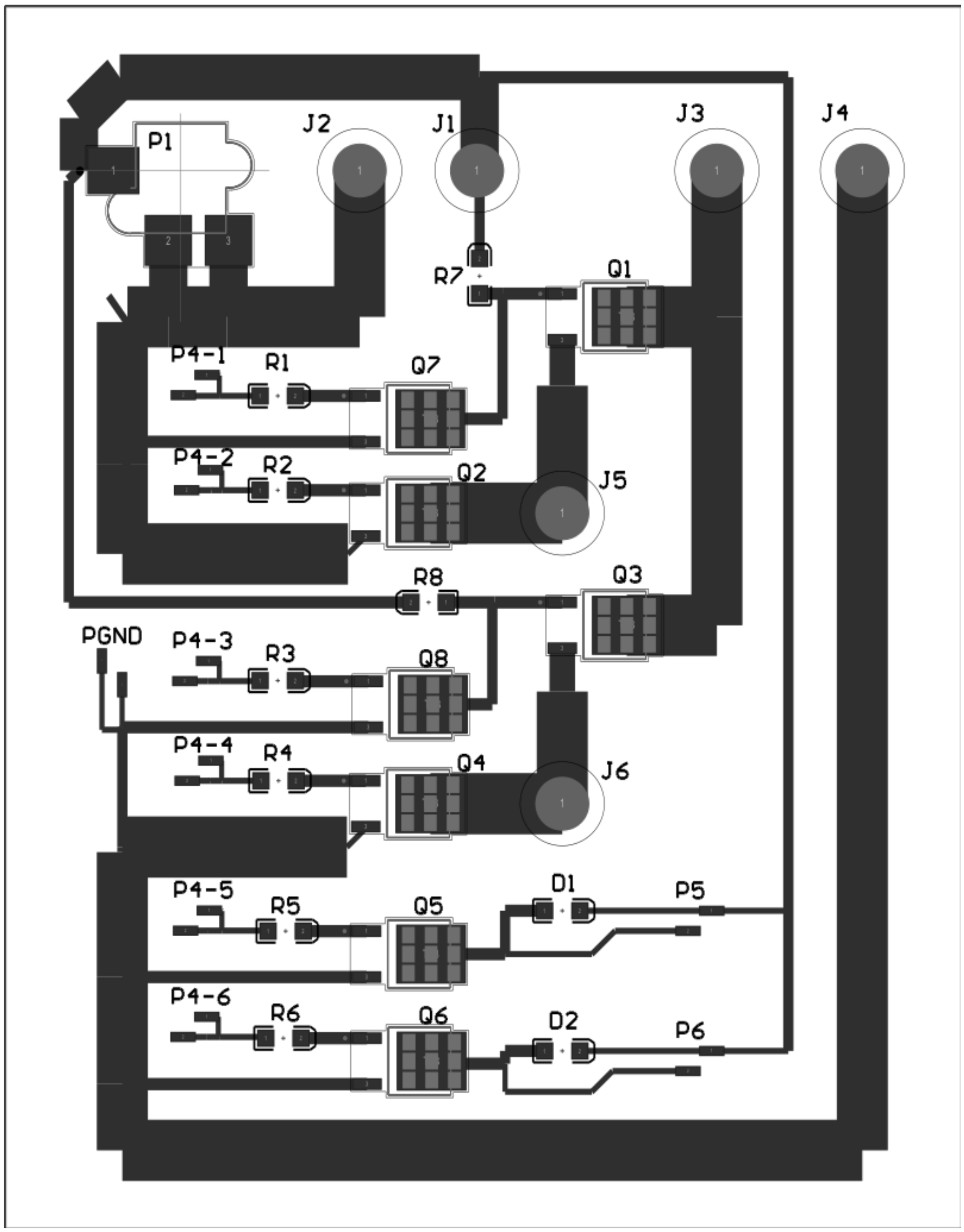

Figure B-7: Final Charging Circuit PCB

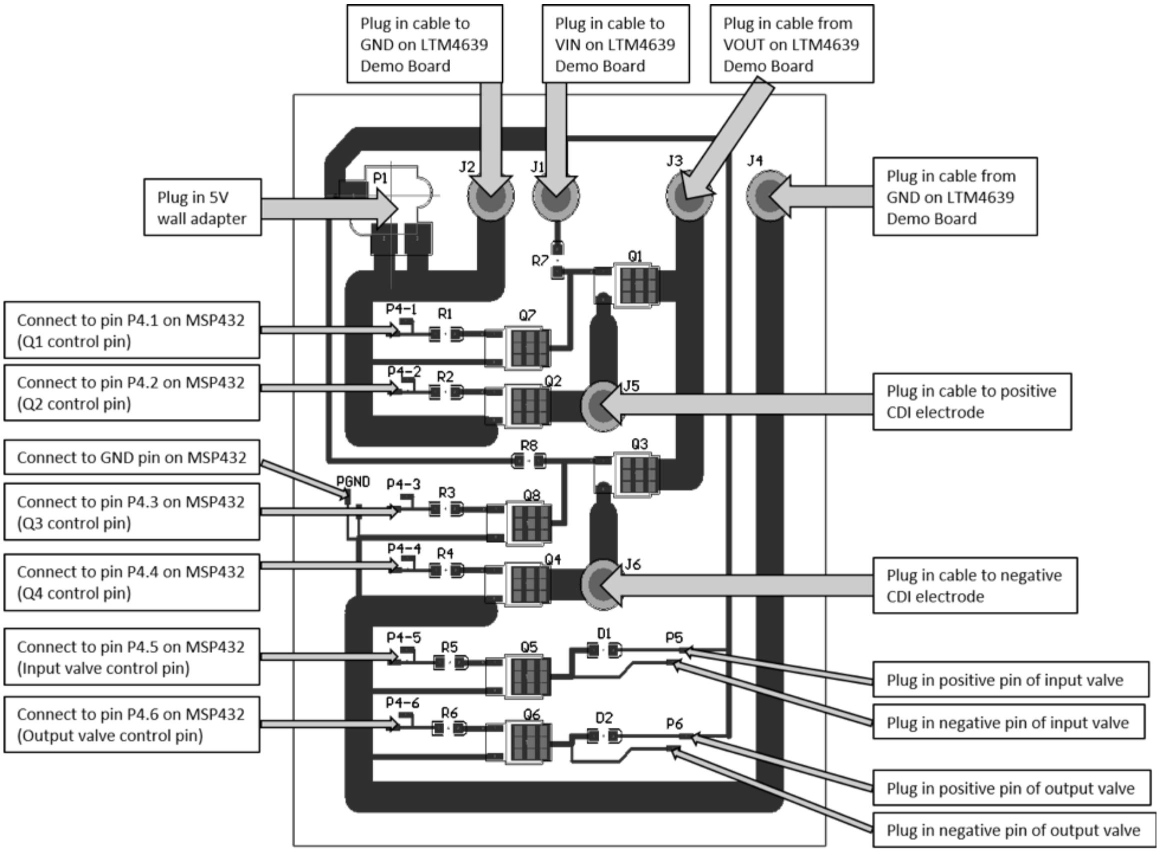

Figure B-8: PCB Connections

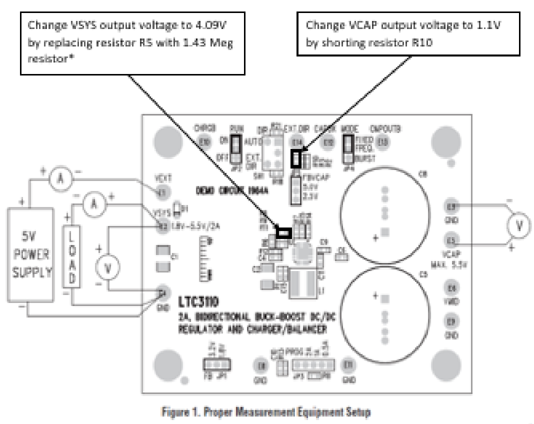

Figure B-9: Changes to LTC3110 Demo Board

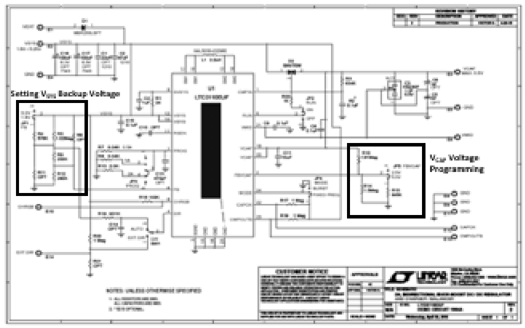

Figure B-10: LTC3110 Demo Board Schematic

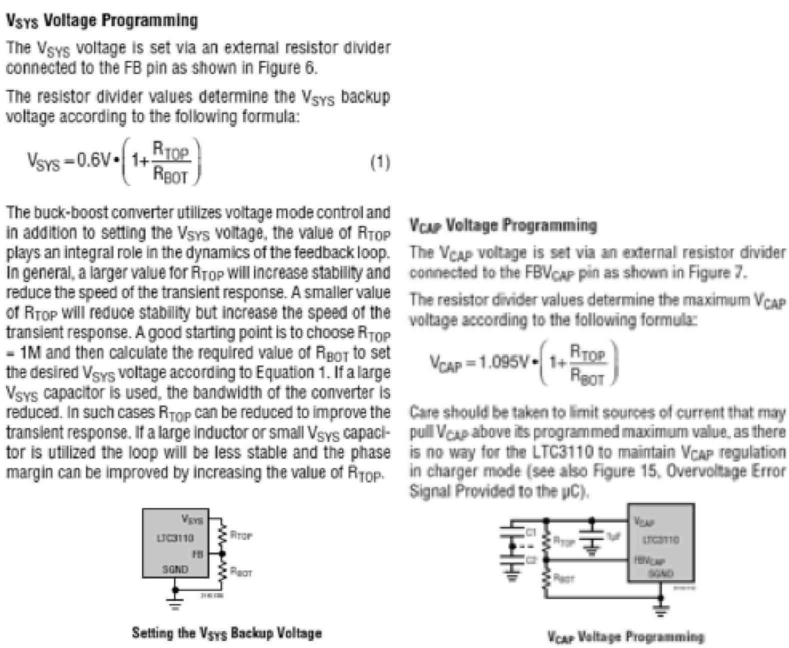

V_{SYS} Voltage Programming

The V_{SYS} voltage is set via an external resistor divider connected to the FB pin as shown in Figure 6.

The resistor divider values determine the V_{SYS} backup voltage according to the following formula:

$$V_{SYS} = 0.6V \cdot \left(1 + \frac{R_{TOP}}{R_{BOT}}\right) \quad (1)$$

The buck-boost converter utilizes voltage mode control and in addition to setting the V_{SYS} voltage, the value of R_{TOP} plays an integral role in the dynamics of the feedback loop. In general, a larger value for R_{TOP} will increase stability and reduce the speed of the transient response. A smaller value of R_{TOP} will reduce stability but increase the speed of the transient response. A good starting point is to choose R_{TOP} = 1M and then calculate the required value of R_{BOT} to set the desired V_{SYS} voltage according to Equation 1. If a large V_{SYS} capacitor is used, the bandwidth of the converter is reduced. In such cases R_{TOP} can be reduced to improve the transient response. If a large inductor or small V_{SYS} capacitor is utilized the loop will be less stable and the phase margin can be improved by increasing the value of R_{TOP}.

Setting the V_{SYS} Backup Voltage

V_{CAP} Voltage Programming

The V_{CAP} voltage is set via an external resistor divider connected to the FBV_{CAP} pin as shown in Figure 7.

The resistor divider values determine the maximum V_{CAP} voltage according to the following formula:

$$V_{CAP} = 1.095V \cdot \left(1 + \frac{R_{TOP}}{R_{BOT}}\right)$$

Care should be taken to limit sources of current that may pull V_{CAP} above its programmed maximum value, as there is no way for the LTC3110 to maintain V_{CAP} regulation in charger mode (see also Figure 15, Overvoltage Error Signal Provided to the µC).

V_{CAP} Voltage Programming

Figure B-11: LTC3110 Voltages from datasheet

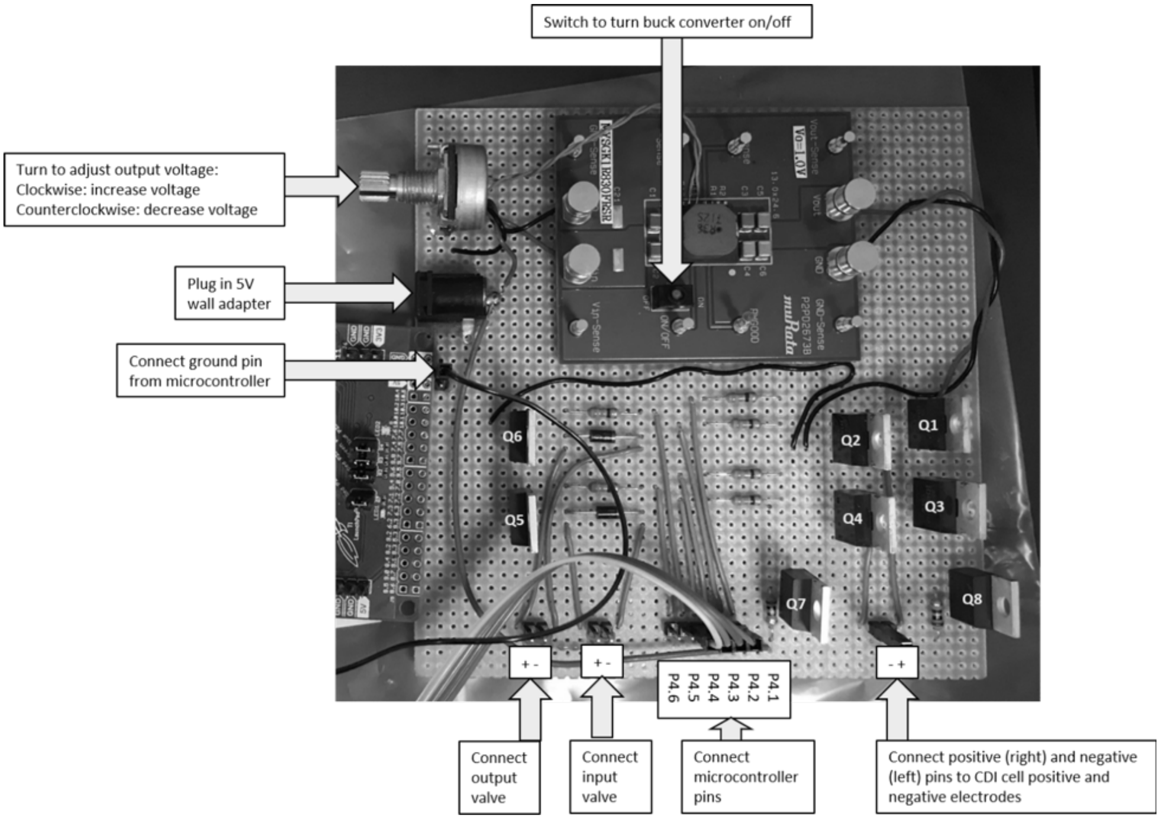

Figure B-12: Prototype circuit on protoboard

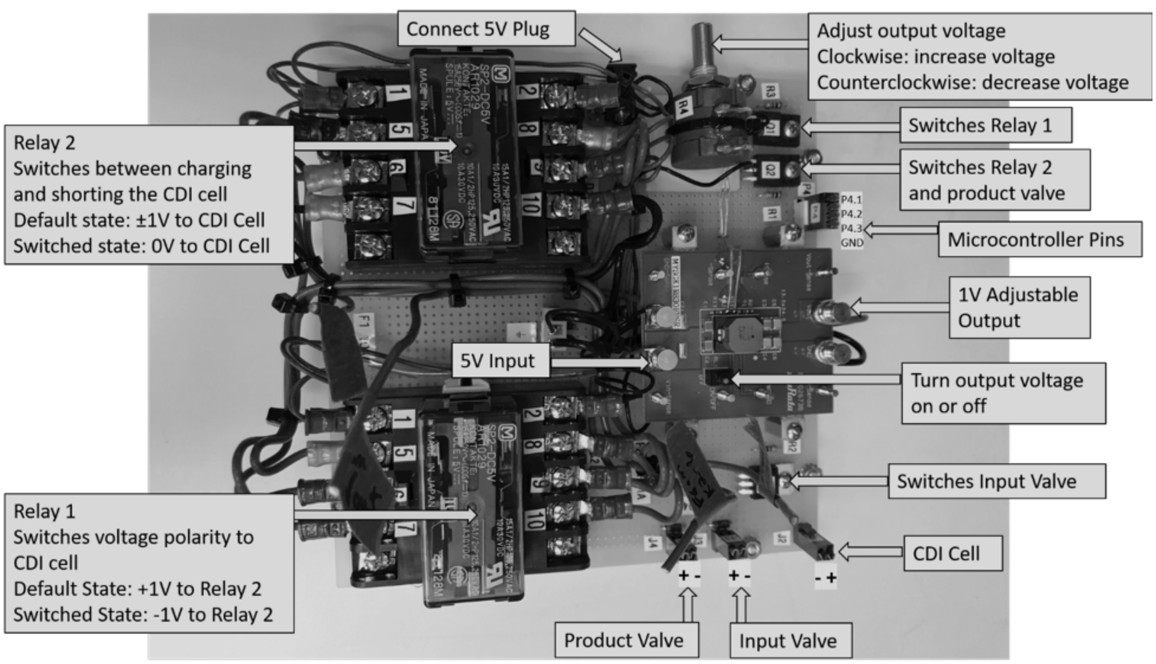

Figure B-13: Previous Prototype Circuit with Relays

Appendix C

Code

C.1 main.c

```
// Preprocessor Directives
// Header Files
#include "msp432p401r.h"
#include "initialize.h"
#include "UARTCom.h"
// Global Variables
#define ON 1
#define OFF 0

// Function Declarations
void delaySeconds(float seconds);
void FET1(int state);
void FET2(int state);
void FET3(int state);
void FET4(int state);
void FET5(int state);
void FET6(int state);
```

```
// Main
void main(void){
    // initialization off all peripherals
    initializeCore();
    initializeTimer32_1();
    initializeUART_A2();
    __enable_interrupts(); // enable NVIC global interrupts

    // Initialize to 0V
    FET1(OFF);
    FET2(ON);
    FET3(OFF);
    FET4(ON);
    // Initial output valve to brine
    FET5(OFF);
    FET6(ON);

    // Auto-start if S1 pushed at startup
    if ((P1->IN & BIT1) != BIT1){
        goState = 3;
    }

    // Main loop
    while(1){
        // sleep when system is idle
        // until receive command for
        // desal state
        while (goState == 0) {
            sleepFlag=0;
```

```
    __sleep();
    status = 0;
}

switch (goState) {
    case 3 :{ // +1V, 0V, -1V voltage cycle
        for (cycleIndex = 0;
        cycleIndex < numberCycles;
        cycleIndex++){
            // +1V (Q1 and Q4 on)
            FET4(ON);
            FET2(OFF);
            FET3(OFF);
            FET1(ON);
            // output valve to product
            FET6(OFF);
            delaySeconds(oneVoltTime);

            // 0V (Q2 and Q4 on)
            FET1(OFF);
            FET2(ON);
            // input valve slow
            FET5(ON);
            // output valve to brine
            FET6(ON);
            delaySeconds(slowFlowTime);
            // input valve fast
            FET5(OFF);
            delaySeconds(zeroVoltTime-slowFlowTime);
```

```
            // -1V (Q2 and Q3 on)
            FET4(OFF);
            FET3(ON);
            // output valve to product
            FET6(OFF);
            delaySeconds(oneVoltTime);

            // 0V (Q2 and Q4 on)
            FET3(OFF);
            FET4(ON);
            // input valve slow
            FET5(ON);
            // output valve to brine
            FET6(ON);
            delaySeconds(slowFlowTime);
            // input valve fast
            FET5(OFF);
            delaySeconds(zeroVoltTime-slowFlowTime);

            //exit loop if stop has been requested
            if (goState==0)
                break;
        }
        // no command currently being processed
        goState = 0;
        break;
    }
    default :{
        goState = 0;
        status = 0;
```

```
                break;
            }
        }
    }
}

// Function Definitions

// This function creates delays
//  using the 32-bit timer peripheral.
// The timer runs at 12 MHz,
//  where the input argument
//  to the function is in seconds.
void delaySeconds(float seconds){
    int repeat = seconds / 80;
    int remainder = (int) seconds % 80;
    int i;
    for (i=0; i<repeat; i++){
        sleepFlag = 1;
        // wait for predefined number of seconds
        TIMER32_1->LOAD = (uint32_t) (48000000.0 * 80);
        __sleep(); // wait for interrupt
        while((sleepFlag==1) && (goState!=0))
        {
            __sleep(); // wait for Timer32 interrupt
        }
    }
    if (remainder != 0){
        sleepFlag = 1;
        // wait for predefined number of seconds
```

```
        TIMER32_1->LOAD = (uint32_t)
            (48000000.0 * remainder);
        __sleep(); // wait for interrupt
        while((sleepFlag==1) && (goState!=0))
        {
            __sleep(); // wait for Timer32 interrupt
        }
    }
    if (seconds - (int)(seconds) != 0){
        sleepFlag = 1;
        float frac = seconds - (int)(seconds);
        // wait for predefined number of seconds
        TIMER32_1->LOAD = (uint32_t) (48000000.0 * frac);
        __sleep(); // wait for interrupt
        while((sleepFlag==1) && (goState!=0))
        {
            __sleep(); // wait for Timer32 interrupt
        }
    }
}

// ISR for 32-bit timer
void T32_INT1_IRQHandler(void){
        // clear interrupts
    TIMER32_1->INTCLR = 0;
    sleepFlag = 0;
}

// Control signal for Q1
// Logic is reversed since Q1
```

```
//  is driven by Q7
void FET1(int state){
    if(state==OFF){
        // pin P4.1 high
        P4->OUT |= BIT1;
    }else{
        // pin P4.1 low
        P4->OUT &= ~BIT1;
    }

// Control signal for Q2 gate
void FET2(int state){
    if(state==ON){
        // pin P4.2 high
        P4->OUT |= BIT2;
    }else{
        // pin P4.2 low
        P4->OUT &= ~BIT2;
    }
}

// Control signal for Q3
// Logic is reversed since Q3
//  is driven by Q8
void FET3(int state){
    if(state==OFF){
        // pin P4.3 high
        P4->OUT |= BIT3;
    }else{
        // pin P4.3 low
```

```
            P4->OUT &= ~BIT3;
        }
}

// Control signal for Q4 gate
void FET4(int state){
        if(state==ON){
            // pin P4.4 high
            P4->OUT |= BIT4;
        }else{
            // pin P4.4 low
            P4->OUT &= ~BIT4;
        }
}

// Control signal for Q5 gate
// Input valve slow when on
void FET5(int state){
        if(state==ON)
            // pin P4.5 high
            P4->OUT |= BIT5;
        }else{
            // pin P4.5 low
            P4->OUT &= ~BIT5;
        }
}

// Control signal for Q6 gate
// Output valve to brine
// when on
```

```
void FET6(int state){
    if(state==ON){
        // pin P4.6 high
        P4->OUT |= BIT6;
    }else{
        // pin P4.6 low
        P4->OUT &= ~BIT6;
    }
}
```

Appendix D

Derivations

D.1 Efficiency of Two Capacitor Energy Transfer

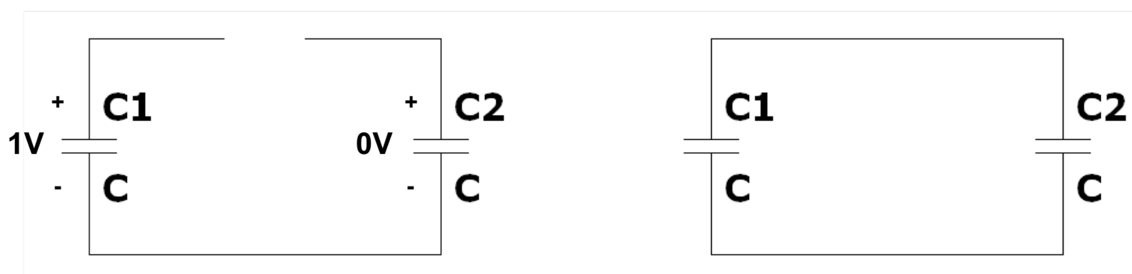

Figure D-1: Initially C1 charged to 1V, C2 charged with 0V

The initial energy, E_i, is calculated with an initial voltage, V_i, across C_1.

$$E_i = \frac{1}{2} C_1 V_i^2 \tag{D.1}$$

The charged capacitor, C_1, initially has a charge Q. When the two capacitors are connected, each capacitor will have a final charge $\frac{1}{2}Q$. The final voltage across the capacitors is calculated using the fact that the final voltage across both capacitors is the same and both have half the initial charge of C_1.

$$V_i = \frac{Q}{C} \tag{D.2}$$

$$V_f = \frac{\frac{1}{2}Q}{C} = \frac{1}{2}V_i \quad \text{(D.3)}$$

The final energy transferred to the initially uncharged capacitor C_2 is calculated at the final energy, E_{C2}, stored in C_2.

$$E_{C2} = \frac{1}{2}C_2V_f^2 \quad \text{(D.4)}$$

The ratio of the energy transferred to the uncharged capacitor relative to the total energy initially available is:

$$\frac{E_{C2}}{E_i} = \frac{\frac{1}{2}C_2V_f^2}{\frac{1}{2}C_1V_i^2} \quad \text{(D.5)}$$

Since both capacitors have the same capacitance, C:

$$\frac{E_{C2}}{E_i} = \frac{\frac{1}{2}CV_f^2}{\frac{1}{2}CV_i^2} \quad \text{(D.6)}$$

Substituting eq. D.3 for V_f:

$$\frac{E_{C2}}{E_i} = \frac{\frac{1}{2}C(\frac{1}{2}V_i)^2}{\frac{1}{2}CV_i^2} \quad \text{(D.7)}$$

$$\frac{E_{C2}}{E_i} = \frac{\frac{1}{8}CV_i^2}{\frac{1}{2}CV_i^2} \quad \text{(D.8)}$$

$$\frac{E_{C2}}{E_i} = \frac{1}{4} \quad \text{(D.9)}$$

Therefore, using this energy transfer method, only 25% of the initial energy stored in the charged capacitor can be transferred to the uncharged capacitor.

The final energy, E_f, of the two capacitor system is calculated in eq. D.10.

$$E_f = \frac{1}{2}C_1V_f^2 + \frac{1}{2}C_2V_f^2 \quad \text{(D.10)}$$

Substituting V_f from eq. D.3:

$$E_f = \frac{1}{2}C_1(\frac{1}{2}V_i)^2 + \frac{1}{2}C_2(\frac{1}{2}V_i)^2 \quad \text{(D.11)}$$

The efficiency, η, of the energy transfer is calculated.

$$\eta = \frac{E_f}{E_i} \tag{D.12}$$

$$\eta = \frac{\frac{1}{2}C_1(\frac{1}{2}V_i)^2 + \frac{1}{2}C_2(\frac{1}{2}V_i)^2}{\frac{1}{2}C_1V_i^2} \tag{D.13}$$

Since both capacitors have the same capacitance, C, eq. D.13 can be simplified.

$$\eta = \frac{\frac{1}{2}C(\frac{1}{2}V_i)^2 + \frac{1}{2}C(\frac{1}{2}V_i)^2}{\frac{1}{2}CV_i^2} \tag{D.14}$$

$$\eta = \frac{C(\frac{1}{2}V_i)^2}{\frac{1}{2}CV_i^2} \tag{D.15}$$

$$\eta = \frac{\frac{1}{4}CV_i^2}{\frac{1}{2}CV_i^2} \tag{D.16}$$

$$\eta = \frac{1}{2} \tag{D.17}$$

So the final energy stored in both capacitors when a charged capacitor is connected to an uncharged capacitor is only half the initial energy stored in the charged capacitor.

Bibliography

[1] H. Bigas, editor. *The Global Water Crisis: Addressing an Urgent Security Issue.* Papers for the InterAction Council, 2011-2012. UNU-INWEH, Hamilton, Canada, 2012.

[2] Michael I. Cameron, Dechen Morisco, Daniel Hofstetter, Erol Uman, Justin Wilkinson, Zachary C. Kennedy, Sean A. Fontenot, William T. Lee, Christopher H. Hendon, and Jamie M. Foster. Systematically improving espresso: Insights from mathematical modeling and experiment. *Matter*, 2(3):631 – 648, 2020.

[3] Raylin Chen, Thomas Sheehan, Jing Lian Ng, Matthew Brucks, and Xiao Su. Capacitive deionization and electrosorption for heavy metal removal. *Environ. Sci.: Water Res. Technol.*, 6:258–282, 2020.

[4] Marc A. Anderson, Ana L. Cudero, and Jesus Palma. Capacitive deionization as an electrochemical means of saving energy and delivering clean water. comparison to present desalination practices: Will it compete? *Electrochimica Acta*, 55(12):3845–3856, April 2010.

[5] X. Gao, A. Omosebi, N. Holubowitch, J. Landon, and K. Liu. Capacitive deionization using alternating polarization: Effect of surface charge on salt removal. *Electrochimica Acta*, 233:249 – 255, 2017.

[6] Junil Kang, Taeyoung Kim, Hojoon Shin, Jiho Lee, Jung-Ik Ha, and Jeyong Yoon. Direct energy recovery system for membrane capacitive deionization. *Desalination*, 398:144–150, November 2016.

[7] Christopher H. Hendon, Lesley Colonna-Dashwood, and Maxwell Colonna-Dashwood. The role of dissolved cations in coffee extraction. *Journal of Agricultural and Food Chemistry*, 62(21):4947–4950, 2014. PMID: 24802110.

[8] M. Alkuran, Mohamed Orabi, and Norman Scheinberg. Highly efficient capacitive de-ionization (cdi) water purification system using a buck-boost converter. *Twenty-Third Annual IEEE Applied Power Electronics Conference and Exposition*, 2008.

[9] Matthew E. Suss, Theodore F. Baumann, William L. Bourcier, Christopher M. Spadaccini, Klint A. Rose, Juan G. Santiago, and Michael Stadermann. Capacitive desalination with flow-through electrodes. *Energy and Environmental Science*, 5(11):9511–9519, 2012.

[10] Steven A. Hawks, Maira R. Cerón, Diego I. Oyarzun, Tuan Anh Pham, Cheng Zhan, Colin K. Loeb, Daniel Mew, Amanda Deinhart, Brandon C. Wood, Juan G. Santiago, Michael Stadermann, and Patrick G. Campbell. Using ultramicroporous carbon for the selective removal of nitrate with capacitive deionization. *Environmental Science & Technology*, 53(18):10863–10870, June 2019.

[11] Atlantis Technologies. Technical summary radial deionization ™ *Low Cost Waste Water Desalination.* White paper, Atlantis Technologies, 2012.

[12] Voltea. Technology comparison. Voltea's technical bulletin, Voltea, 2015.